Article

Current Biology

LysM-mediated signaling in *Marchantia polymorpha* highlights the conservation of pattern-triggered immunity in land plants

Highlights

- Chitin and peptidoglycan trigger immune responses in *Marchantia polymorpha*
- MpLYK1 and MpLYR are required for sensing chitin and peptidoglycan fragments
- MpLYK1 contributes to defense against fungal and bacterial pathogens
- Phosphoproteomics identifies MpPHOT as a novel player in pattern-triggered immunity

Authors

Izumi Yotsui, Hidenori Matsui, Shingo Miyauchi, ..., Takashi Ueda, Takayuki Kohchi, Hirofumi Nakagami

Correspondence

nakagami@mpipz.mpg.de

In brief

Pattern-triggered immunity is the first line of inducible defense in angiosperms. Yotsui et al. demonstrate that lysin motif (LysM)-domain-containing receptor-mediated pattern-triggered immunity for defense against fungal and bacterial pathogens is conserved in the liverwort *Marchantia polymorpha*.

Yotsui et al., 2023, Current Biology *33*, 1–15
September 11, 2023
https://doi.org/10.1016/j.cub.2023.07.068

CellPress

Current Biology

CellPress

Article

LysM-mediated signaling in *Marchantia polymorpha* highlights the conservation of pattern-triggered immunity in land plants

Izumi Yotsui,[1,2] Hidenori Matsui,[1,3] Shingo Miyauchi,[4,5] Hidekazu Iwakawa,[4,6] Katharina Melkonian,[4] Titus Schlüter,[4] Santiago Michavila,[7] Takehiko Kanazawa,[8,9] Yuko Nomura,[1] Sara Christina Stolze,[4] Hyung-Woo Jeon,[4] Yijia Yan,[4] Anne Harzen,[4] Shigeo S. Sugano,[10] Makoto Shirakawa,[11,12] Ryuichi Nishihama,[11,13] Yasunori Ichihashi,[1,14] Selena Gimenez Ibanez,[7] Ken Shirasu,[1] Takashi Ueda,[8,9] Takayuki Kohchi,[11] and Hirofumi Nakagami[1,4,15,16,*]

[1]RIKEN Center for Sustainable Resource Science, Yokohama 230-0045, Kanagawa, Japan
[2]Department of BioScience, Tokyo University of Agriculture, Setagaya, Tokyo 156-8502, Japan
[3]Graduate School of Environmental and Life Sciences, Okayama University, Okayama 700-8530, Japan
[4]Max Planck Institute for Plant Breeding Research, 50829 Cologne, Germany
[5]Okinawa Institute of Science and Technology Graduate University, Onna 904-0495, Okinawa, Japan
[6]School of Biological Science and Technology, College of Science and Engineering, Kanazawa University, Kakuma-machi, Kanazawa 920-1192, Ishikawa, Japan
[7]Department of Plant Molecular Genetics, Centro Nacional de Biotecnología, Consejo Superior de Investigaciones Científicas (CNB-CSIC), 28049 Madrid, Spain
[8]Division of Cellular Dynamics, National Institute for Basic Biology, Nishigonaka 38, Myodaiji, Okazaki 444-8585, Aichi, Japan
[9]Department of Basic Biology, SOKENDAI (The Graduate University for Advanced Studies), Nishigonaka 38, Myodaiji, Okazaki 444-8585, Aichi, Japan
[10]Bioproduction Research Institute, The National Institute of Advanced Industrial Science and Technology (AIST), Tsukuba 305-8566, Ibaraki, Japan
[11]Graduate School of Biostudies, Kyoto University, Kyoto 606-8502, Japan
[12]Division of Biological Science, Graduate School of Science and Technology, Nara Institute of Science and Technology (NAIST), Ikoma 630-0192, Nara, Japan
[13]Department of Applied Biological Science, Faculty of Science and Technology, Tokyo University of Science, Noda 278-8510, Chiba, Japan
[14]RIKEN BioResource Research Center, Tsukuba 305-0074, Ibaraki, Japan
[15]Twitter: @Grandpa_Hiro
[16]Lead contact
*Correspondence: nakagami@mpipz.mpg.de
https://doi.org/10.1016/j.cub.2023.07.068

SUMMARY

Pattern-recognition receptor (PRR)-triggered immunity (PTI) wards off a wide range of pathogenic microbes, playing a pivotal role in angiosperms. The model liverwort *Marchantia polymorpha* triggers defense-related gene expression upon sensing components of bacterial and fungal extracts, suggesting the existence of PTI in this plant model. However, the molecular components of the putative PTI in *M. polymorpha* and the significance of PTI in bryophytes have not yet been described. We here show that *M. polymorpha* has four lysin motif (LysM)-domain-containing receptor homologs, two of which, LysM-receptor-like kinase (LYK) MpLYK1 and LYK-related (LYR) MpLYR, are responsible for sensing chitin and peptidoglycan fragments, triggering a series of characteristic immune responses. Comprehensive phosphoproteomic analysis of *M. polymorpha* in response to chitin treatment identified regulatory proteins that potentially shape LysM-mediated PTI. The identified proteins included homologs of well-described PTI components in angiosperms as well as proteins whose roles in PTI are not yet determined, including the blue-light receptor phototropin MpPHOT. We revealed that MpPHOT is required for negative feedback of defense-related gene expression during PTI. Taken together, this study outlines the basic framework of LysM-mediated PTI in *M. polymorpha* and highlights conserved elements and new aspects of pattern-triggered immunity in land plants.

INTRODUCTION

In angiosperms, cell-surface-localized pattern-recognition receptors (PRRs) recognizing microbe-derived or plant-endogenous molecules play central roles in various plant-microbe interactions, which can be beneficial, neutral, or detrimental.[1] PRRs recognize slowly evolving microbe-associated molecular patterns (MAMPs) or symbiotic signals such as rhizobial nodulation (Nod) factors and mycorrhizal (Myc) factors. PRRs are transmembrane kinases or membrane-associated proteins that function together with kinases, triggering phosphorylation and/or interaction-dependent signaling to activate pattern-triggered

Please cite this article in press as: Yotsui et al., LysM-mediated signaling in *Marchantia polymorpha* highlights the conservation of pattern-triggered immunity in land plants, Current Biology (2023), https://doi.org/10.1016/j.cub.2023.07.068

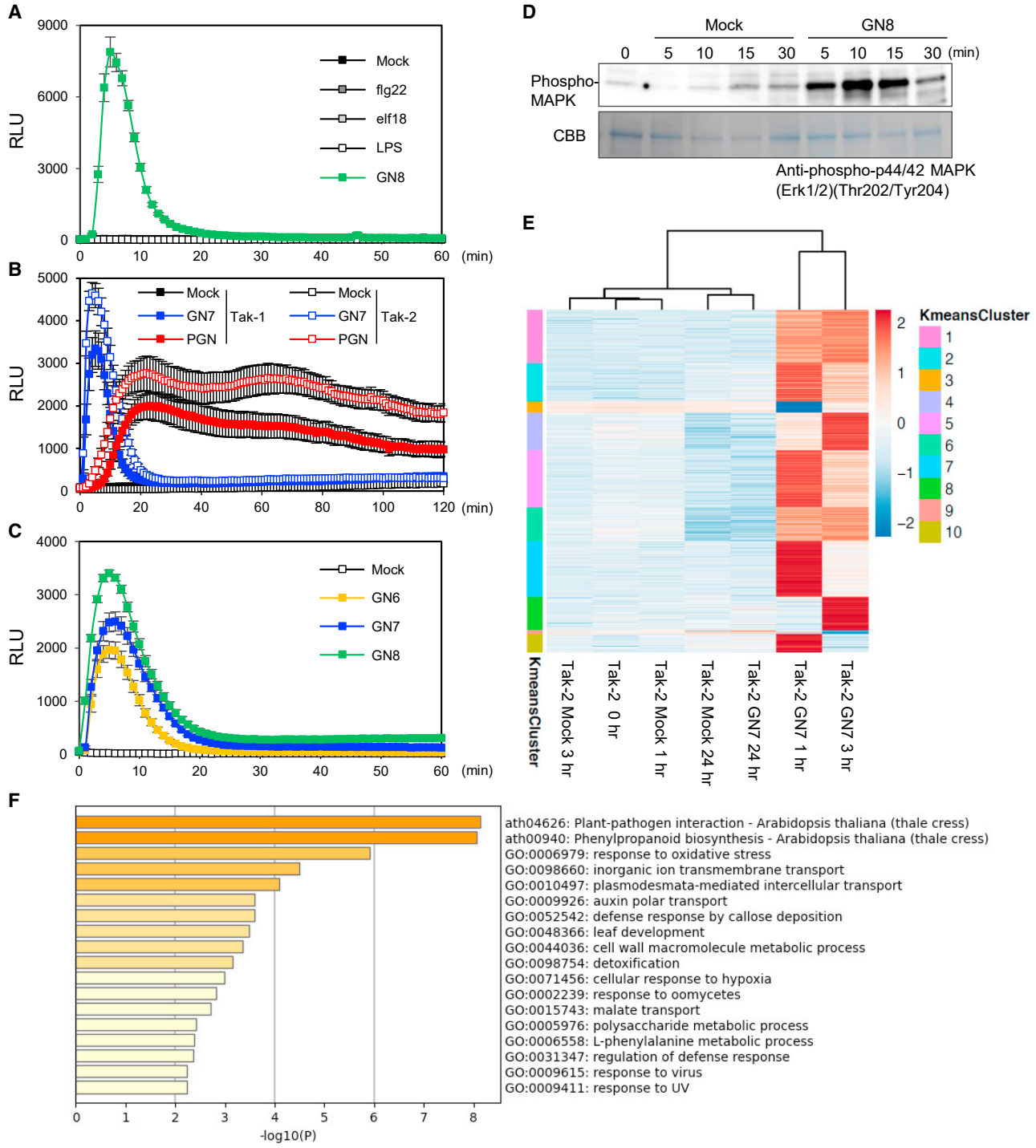

Figure 1. MAMP responses in *M. polymorpha*

(A–C) MAMP-induced reactive oxygen species (ROS) production in Tak-1 (male wild type) and Tak-2 (female wild type). ROS production after MAMP treatment was measured by chemiluminescence mediated by L-012 in 6-day-old gemmalings. The values represent the average and SEs of four replicates.

(A) Wild-type gemmalings were treated with mock (water), 1 μM flg22, 1 μM elf18, 100 μg/mL lipopolysaccharide (LPS) derived from *Pseudomonas aeruginosa*, or 1 μg/mL N-acetylchitooctaose (GN8) with horseradish peroxidase (HRP).

(B) Wild-type gemmalings were treated with mock (water), 1 μM N-acetylchitoheptaose (GN7), or 500 μg/mL peptidoglycan (PGN) derived from *Bacillus subtilis*.

(C) Wild-type gemmalings were treated with mock (water), 1 μM N-acetylchitohexaose (GN6), GN7, or GN8.

(legend continued on next page)

Please cite this article in press as: Yotsui et al., LysM-mediated signaling in *Marchantia polymorpha* highlights the conservation of pattern-triggered immunity in land plants, Current Biology (2023), https://doi.org/10.1016/j.cub.2023.07.068

immunity (PTI) or to initiate symbiosis.[1] Activation of PRRs typically induces a series of characteristic responses, including reactive oxygen species (ROS) production, MAP kinase (MAPK) activation, calcium influx, callose deposition, defense-related gene expression, and growth inhibition.[2]

Well-studied bacterial MAMP receptors such as *Arabidopsis thaliana* AtFLS2 and AtEFR belong to the subfamily XII of leucine-rich repeat receptor-like kinases (LRR-RLKs). AtFLS2 and AtEFR recognize peptide fragments derived from bacterial flagellin and elongation factor Tu (EF-Tu), respectively.[3,4] These LRR-RLK subfamily XII MAMP receptors typically require SERK co-receptors belonging to the subfamily II of LRR-RLKs for downstream signaling.[5,6] In *A. thaliana*, AtBAK1/AtSERK3 functions as a co-receptor for AtFLS2 and AtEFR as well as the brassinosteroid receptor AtBRI1, and it thereby regulates not only PTI but also plant growth and development.[7]

Lysin motif (LysM)-domain-containing receptors (LysM receptors) perceive N-acetylglucosamine (GlcNAc) derivatives from bacteria, fungi, and oomycetes, which can be either MAMPs or symbiotic signals.[1] LysM receptors can be roughly classified into LYK (LysM-RLK), LYR (LYK-related, LysM-RLK without classically conserved kinase domain), and LYP (LysM receptor-like protein, membrane-anchored LysM protein).[8,9] As major cell wall components, bacterial peptidoglycans (PGNs) and fungal chitin oligosaccharides are recognized as MAMPs by LYK, LYR, or LYP to activate PTI.[8] In *A. thaliana*, chitin is perceived by LYR AtLYK5 and LYK AtCERK1, and PGN is perceived by LYP AtLYM1/3 and LYK AtCERK1.[10–12] At*cerk1* mutants are shown to be hyper-susceptible toward fungal pathogens and the pathogenic bacterium *Pseudomonas syringae* pv. *tomato* DC3000 (*Pto* DC3000).[10,11,13] In rice, different combinations of LysM receptors perceive chitin and PGN.[14–16] In either case, LYK CERK1 most likely functions as a co-receptor as do the subfamily II LRR-RLK SERKs for the subfamily XII LRR-RLKs. Importantly, Nod and Myc factors are also perceived by LysM proteins to ensure beneficial symbiotic interactions. In *Lotus japonicus* and *Medicago truncatula*, different CERK1 homologs, most likely originating from gene duplications, function independently for PTI and symbiosis.[17] Intriguingly, however, rice LYK OsCERK1 is involved in both PTI and arbuscular mycorrhizal (AM) symbiosis.[18–20]

Considering the importance of PRRs in angiosperms for communication with various microbes, it is possible that acquisition and diversification of PRRs and their downstream signaling networks played a key role during plant terrestrialization and evolution. Homologs of characterized PRRs can be found in genomes of bryophytes and the charophyte alga *Chara braunii*.[21–25] The moss *Physcomitrium patens* has been shown to sense chitin and PGN fragments in a LYK PpCERK1-dependent manner.[26] The liverwort *Marchantia polymorpha* is able to sense bacterial and fungal extracts, although the molecular components and mechanisms of this sensing are not yet described.[27,28] Here, we identify LysM receptor homologs responsible for chitin- and PGN-induced responses in *M. polymorpha*, and we provide evidence that the LysM receptor homolog contributes to resistance against bacterial and fungal pathogens in *M. polymorpha*. Furthermore, we characterize the LysM-mediated signaling pathway in *M. polymorpha* by phosphoproteomics.

RESULTS

Marchantia polymorpha recognizes chitin and PGN to induce immune responses

A rapid and transient burst of ROS is a hallmark of PRR activation upon MAMP perception in angiosperms. To investigate the conservation of MAMP recognition, we treated the wild-type *M. polymorpha* strains Tak-1 (male) and Tak-2 (female) with the known MAMPs flg22, elf18, chitin, PGN, and lipopolysaccharide (LPS), which trigger ROS burst in *A. thaliana*. Chitin and PGN fragments, but not the other MAMPs, induced ROS burst in *M. polymorpha* (Figures 1A and 1B). In angiosperms and moss, LysM receptors are indispensable for sensing chitin and PGN. As in the case of angiosperms, long-chain chitin oligosaccharides induced stronger ROS burst (Figure 1C). Chitin treatment further induced MAPK activation, which was monitored by the use of an anti-p44/42-ERK antibody (α-pTEpY), as well as *WRKY* gene expression (Figures 1D and S1C). These observations imply that LysM receptor-mediated MAMP perception and signaling mechanisms are conserved in *M. polymorpha*. We then investigated the chitin-induced transcriptional response in *M. polymorpha* Tak-2. Significant transcriptional reprogramming was observed 1 and 3 h after chitin treatment (Figure 1E), and the transient nature of this response was similar to the chitin response in *A. thaliana* (Figure S1A). Gene ontology (GO) analysis of differentially expressed genes (DEGs; $|\log_2 FC| > 2$, adjusted $p < 0.05$) revealed that chitin treatment significantly and primarily induces expression of defense-related genes in *M. polymorpha* (Figure 1F; Data S1M–S1O), as in *A. thaliana* (Figure S1B; Data S1P–S1R). Collectively, these results suggest the existence of a LysM-mediated immune signaling pathway in *M. polymorpha*.

MpLYK1 and MpLYR are responsible for chitin and PGN responses in *M. polymorpha*

BLAST search identified four LysM receptor homologs—two LYKs, one LYR, and one LYP—in the genome of *M. polymorpha*. Phylogenetic analysis of the LysM domains of LysM receptor homologs in selected plant species, covering hornworts, liverwort, mosses, lycophyte, angiosperms, and streptophyte algae (Data S1A and S1B), revealed that the LysM domains of embryophytes form four major clades, i.e., LYKa, LYKb, LYR, and LYP (Figures 2A and S3A). We found single *M. polymorpha* genes in each of the four clades—Mp*LYK1* (LYKa), Mp*LYK2* (LYKb), Mp*LYR*,

(D) GN8-induced MAPK activation in Tak-1. Tak-1 gemmalings were treated with mock (water) or 1 μg/mL GN8 for the indicated times. Activated MAPKs were detected by immunoblotting using anti-p44/42 MAPK antibody.
(E) Clusters of *M. polymorpha* DEGs. Tak-2 0 h stands for before mock (water) or GN7 treatments. Significantly differentially expressed genes with over ±2 $\log_2$ fold changes (false discovery rate [FDR]-adjusted $p < 0.05$) were grouped based on K-means clustering. K-means cluster ID is shown on the left bar. $\log_2$ read count of genes was normalized into the range of ±2. See Data S1M.
(F) Enriched GO terms in the *M. polymorpha* DEGs (E). See Data S1N and S1O.
See also Figure S1.

Please cite this article in press as: Yotsui et al., LysM-mediated signaling in *Marchantia polymorpha* highlights the conservation of pattern-triggered immunity in land plants, Current Biology (2023), https://doi.org/10.1016/j.cub.2023.07.068

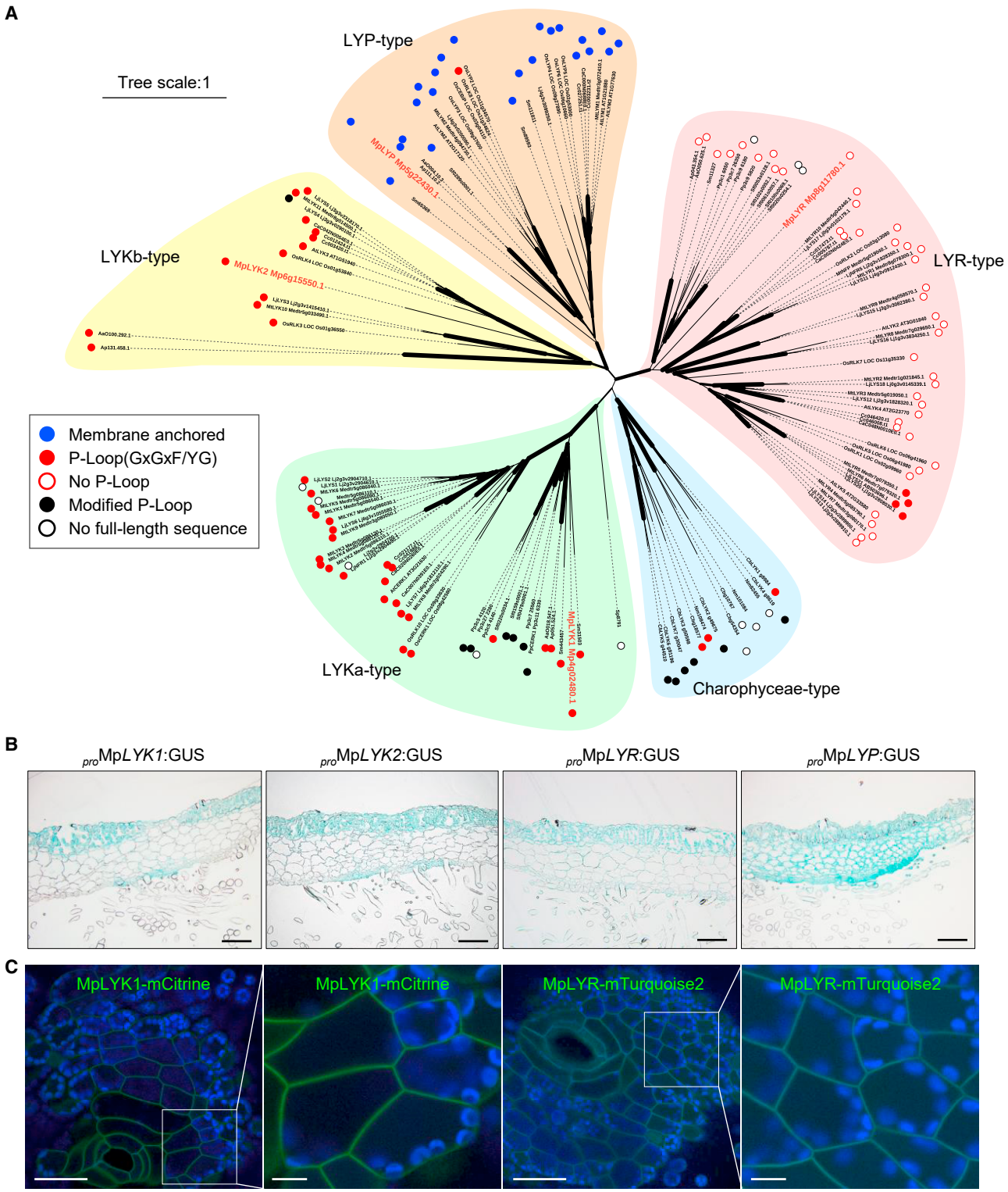

Figure 2. LysM receptor homologs in *M. polymorpha*

(A) Unrooted phylogenetic tree of LysM proteins in plants. Amino acid sequences of ectodomain including LysM1, LysM2, and LysM3 domain were used for drawing the tree. A graphical view of the tree has been generated using iTOL. Width of branches denotes bootstrap support based on 1,000 repetitions. Major subgroups were designated as LYKa, LYKb, LYR, LYP, and Charophyceae type. The proteins containing the basic P-loop (GxGxF/YG) or no P-loop are shown by red circles or red flames, respectively. The proteins containing modified P-loops (see Data S1B) or no full-length sequences in the databases are shown by black

(legend continued on next page)

Please cite this article in press as: Yotsui et al., LysM-mediated signaling in *Marchantia polymorpha* highlights the conservation of pattern-triggered immunity in land plants, Current Biology (2023), https://doi.org/10.1016/j.cub.2023.07.068

CellPress

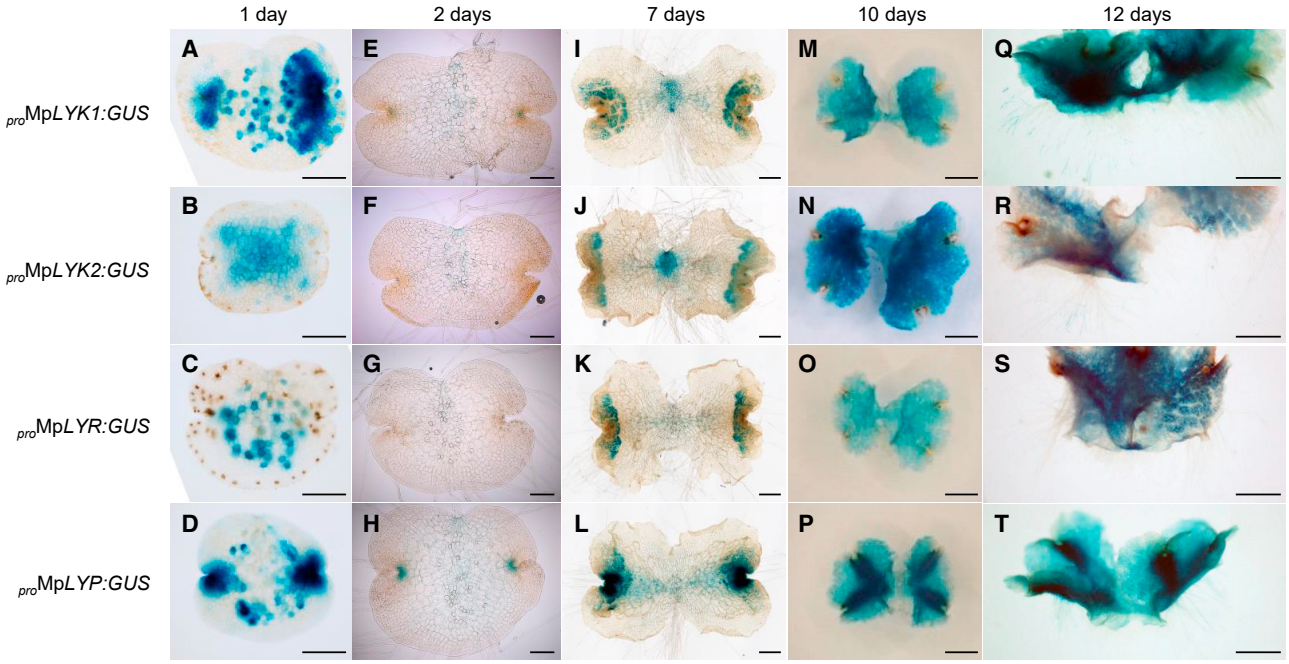

Figure 3. Expression profiles of Mp*LysM* genes GUS-staining images of plants harboring $_{pro}$Mp*LYK1:GUS*, $_{pro}$Mp*LYK2:GUS*, $_{pro}$Mp*LYR:GUS*, and $_{pro}$Mp*LYP:GUS*.

(A–D) 1-day-old gemmalings.
(E–H) 2-day-old gemmalings.
(I–L) 7-day-old gemmalings.
(M–P) 10-day-old thalli, dorsal side.
(Q–T) 12-day-old thalli with rhizoids.
Scale bars, 200 μm (A–H), 500 μm (I–L), and 2 mm (M–T).

and Mp*LYP*—which is in clear contrast to the moss *P. patens* that lacks *LYP* and *LYKb* but has instead evolved to harbor additional copies of *LYKa* and *LYR* (Figures 2A and S2; Data S1A). This suggests that *M. polymorpha* is a useful bryophyte model for comprehensive study of the function and molecular evolution of LysM receptors. MpLYK1 is orthologous to AtCERK1, MpLYK2 is orthologous to AtLYK3, and MpLYR is orthologous to AtLYK4 and AtLYK5 (Figures 2A and S3A). LysM domains from Charophyceae, *Chara braunii* and *Nitella mirabilis*, formed another independent clade (Figures 2A and S3A; Data S1A). It is possible that embryophyte LysM receptors were derived from a LysM receptor in the algal ancestor of embryophytes.

To investigate the contribution of LysM receptor homologs to chitin and PGN responses in *M. polymorpha*, we established disruptant mutants by homologous recombination or CRISPR-Cas9-based genome editing (Figure S5). Obvious developmental defects were not observed for the disruptant mutants under our standard growth conditions. Both chitin- and PGN-induced ROS bursts were abolished in Mp*lyk1*^{ko} and Mp*lyr*^{ge} mutants but not in Mp*lyk2*^{ko} and Mp*lyp*^{ko} mutants (Figures 4A, 4B, and S6), which could be restored by expression of MpLYK1 and MpLYR under their own promoters in the respective mutants (Figures 4A, 4B, S5E, and S6). Likewise, in the Mp*lyk1*^{ko} and Mp*lyr*^{ge} mutants, chitin-induced expression of defense-related genes, selected from the transcriptome data, was abolished (Figure 4C). Subcellular localization of fluorescent protein-tagged MpLYK1 and MpLYR indicated roles at the cell surface (Figures 2C and S4). These results suggest that MpLYK1 and MpLYR function together to sense chitin and PGN and to activate intercellular signaling, leading to defense-related gene expression.

circles or black flames, respectively. The membrane-anchored-type proteins are shown by blue circles. *M. polymorpha* proteins are highlighted in red letters. At, *Arabidopsis thaliana*; Mt, *Medicago truncatula*; Lj, *Lotus japonicus*; Os, *Oryza sativa*; Ca, *Cuscuta australis*; Cc, *Cuscuta campestris*; Sm, *Selaginella moellendorffii*; Sf, *Sphagnum fallax*; Pp, *Physcomitrium patens*; AaO, *Anthoceros agrestis* (Oxford); Ap, *Anthoceros punctatus*; Mp, *Marchantia polymorpha*; Nm, *Nitella mirabilis*; Cb, *Chara braunii*; Sp, *Spirogyra pratensis*.
(B) GUS-staining images of 10-day-old thalli harboring $_{pro}$Mp*LYK1:GUS*, $_{pro}$Mp*LYK2:GUS*, $_{pro}$Mp*LYR:GUS*, and $_{pro}$Mp*LYP:GUS*, respectively. The section is between the dorsal side and the ventral side containing the air chamber. Scale bars, 200 μm.
(C) Plasma membrane localization of MpLYK1-mCitrine and MpLYR-mTurquoise2. Magnified images of the boxed regions are also shown. Single confocal images of *M. polymorpha* thallus cells expressing MpLYK1-mCitrine or MpLYR-mTuquoise2. Green, cyan, and blue pseudo-colors indicate the fluorescence from mCitrine, mTurquoise2, and chlorophyll, respectively. Scale bars, 50 μm in wide images and 10 μm in magnified images. Note that the cell wall of air pore cells emitted autofluorescence, which is difficult to distinguish from the fluorescence of mTurquoise2 in our experimental condition (Figure S4).
See also Figures S2 and S3.

Please cite this article in press as: Yotsui et al., LysM-mediated signaling in *Marchantia polymorpha* highlights the conservation of pattern-triggered immunity in land plants, Current Biology (2023), https://doi.org/10.1016/j.cub.2023.07.068

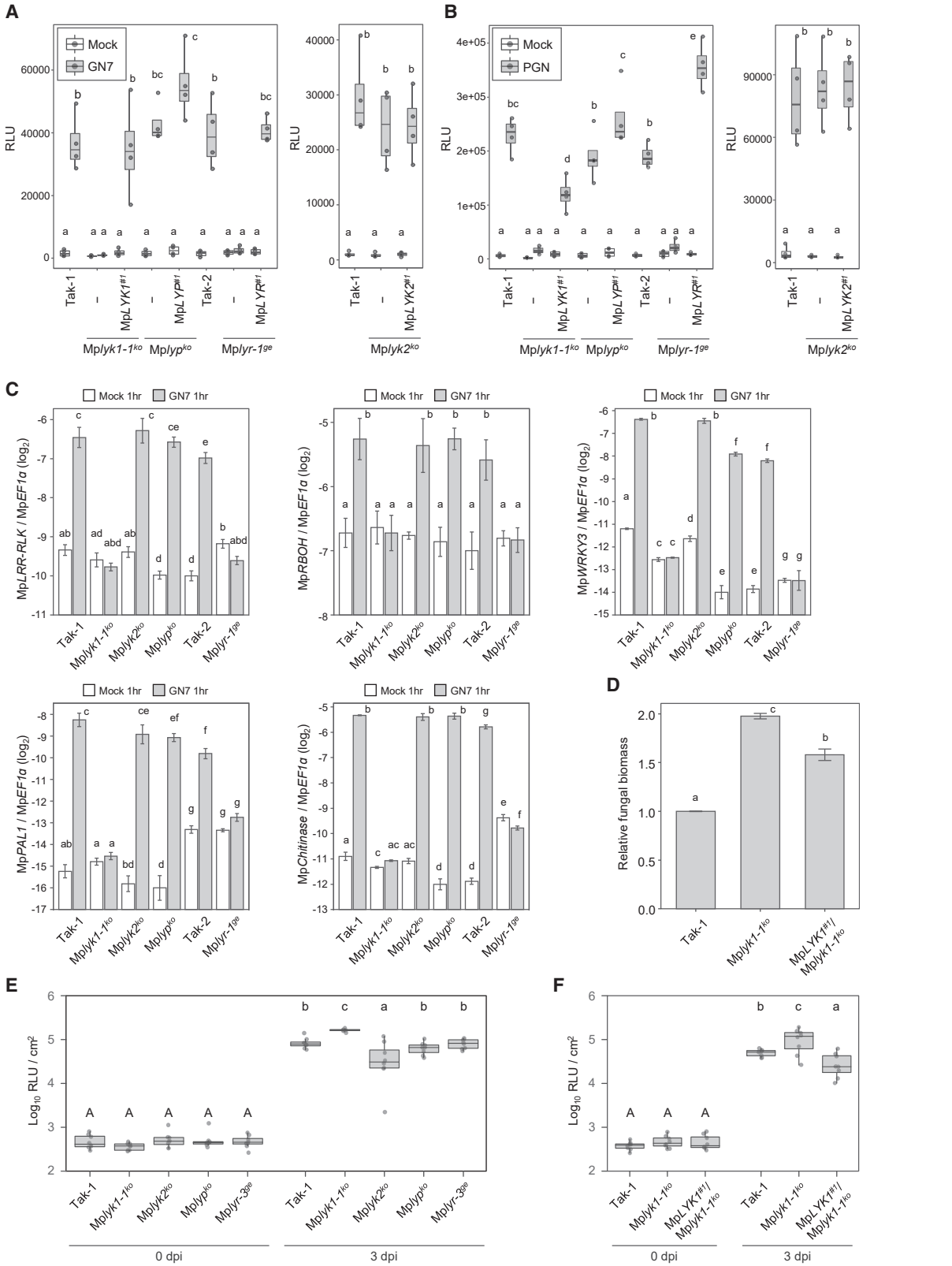

(legend on next page)

Please cite this article in press as: Yotsui et al., LysM-mediated signaling in *Marchantia polymorpha* highlights the conservation of pattern-triggered immunity in land plants, Current Biology (2023), https://doi.org/10.1016/j.cub.2023.07.068

Air chambers have been shown to support colonization by invading microbes in *M. polymorpha*.[29,30] In particular, assimilatory filaments, which are specialized cell types located in air chambers for photosynthesis with less pronounced cuticle coverage, can be primarily targeted by pathogenic microbes.[31] GUS reporter-based promoter analysis indicated that Mp*LYK1* and Mp*LYR* are primarily expressed in assimilatory filaments and upper epidermis (Figures 2B and 3), consistent with their potential roles in PTI in *M. polymorpha*. Indeed, the Mp*lyk1*^{ko} mutant displayed hyper-susceptibility to the pathogenic bacterium *Pto* DC3000 as well as to the pathogenic fungus *Fusarium oxysporum* (*Fo*) f. sp. *lycopersici* 4287 (Fol4287) (Figures 4D–4F). Taken together, our results demonstrate that LysM-mediated PTI is well conserved in the liverwort.

Phosphoproteomic analysis of LysM-mediated signaling pathway in *M. polymorpha*

To explore downstream signaling components of LysM receptors in *M. polymorpha*, we performed differential phosphoproteomics upon chitin treatment. By the use of Mp*lyk1-1*^{ko}, we confirmed that chitin-induced phosphoproteome change in *M. polymorpha* depends largely on MpLYK1 in our experimental conditions (Figure 5; Data S1U–S1Y). In total, we identified 218 protein groups that were phospho-regulated 10 min after chitin treatment (Data S1D–S1G), a time point at which the maximum level of MAPK dual phosphorylation was observed (Figure 1D). As a proof of concept, upon chitin treatment, we observed phospho-regulation of MpLYK1 and MpLYR and the dual phosphorylation of MpMPK1, which is the only MAPK orthologous to AtMPK3, AtMPK4, and AtMPK6 (Figures 6A–6C; Data S1D–S1G).[22] Strikingly, homologs of PTI-related components described in angiosperms are rather comprehensively identified as chitin-induced phospho-regulated proteins (Figures 6A–6C; Data S1D–S1G), which include homologs of receptor-like cytoplasmic kinases (RLCKs), respiratory burst oxidase homolog (RBOH), reduced hyperosmolality-induced [Ca^{2+}] increase (OSCA), MAPK kinase (MAPKK), MAPKK kinase (MAPKKK), MPK phosphatase (MKP), protein phosphatase type 2C (PP2C), WRKY, and calmodulin-binding transcription activator (CAMTA). Secretion- and autophagy-related components were also identified. This finding suggests that the intracellular signaling mechanisms leading to defense responses are also conserved in the liverwort.

Phototropin is required for repressing the induced defense-related genes in *M. polymorpha*

Our phosphoproteome profiling identified various components for which roles in PTI have not yet been described, including the blue-light receptor phototropin MpPHOT (Figure 6A; Data S1D–S1G). Phototropins from various plant species including MpPHOT are known to be activated by blue-light irradiation through induction of auto-phosphorylation, which can be visualized by a phosphorylation-dependent mobility shift on SDS-PAGE.[34] Blue-light irradiation but not chitin treatment induced a mobility shift of MpPHOT (Figure 7A), indicating that these two stimuli induce phosphorylation at different sites on MpPHOT. Indeed, differential phosphoproteomics upon blue-light irradiation revealed that different sites are phosphorylated upon chitin treatment and upon blue-light irradiation (Figure 7B; Data S1H–S1L). To investigate a potential role of MpPHOT in PTI, we compared the chitin-induced transcriptional response of the Mp*phot*^{ko} mutant (female) and wild-type Tak-2 (female). K-mean clustering of DEGs identified a gene group, cluster 6, that is uniquely upregulated in the Mp*phot*^{ko} mutant 24 h after chitin treatment (Figure 7C; Data S1S and S1T). GO analysis of genes in cluster 6 revealed that defense-related genes are upregulated in the Mp*phot*^{ko} mutant (Figure S7). Expression kinetics of the cluster 6 genes indicated that MpPHOT is required for switching off gene expression during recovery from immune activation (Figure 7D). Besides, chitin-induced ROS burst was slightly upregulated in the Mp*phot*^{ko} mutant (Figure 7E). Correspondingly, the Mp*phot*^{ko} mutant displayed enhanced resistance to *Pto* DC3000 (Figure 7F). These results suggest a potential role of phototropin in optimal recovery of plants from unwanted long-term immune activation.

DISCUSSION

PTI plays a vital role in angiosperms, but its significance in bryophytes remains elusive. In the moss *P. patens*, chitin treatment induces MAPK activation, defense-related gene expression, and cell wall modification in a Pp*CERK1*-dependent manner.[26]

Figure 4. MpLYK1 and MpLYR are required for chitin- or PGN-induced responses

(A and B) Chitin- or PGN-induced ROS bursts in LysM receptor homolog disruptants. 6-day-old gemmalings of wild-type plants, disruptants, and complementation lines were treated with mock (water), 1 μM GN7 (A), or 500 μg/mL PGN from *Bacillus subtilis* (B). The boxplot indicates total value of RLU measured by a luminometer for 30 min after GN7 treatment (A) or for 120 min after PGN treatment (B). Boxes show upper and lower quartiles of the value, and lines in boxes represent the medians. Statistical analysis was performed using Student's t test with p values adjusted by the Benjamini-Hochberg (BH) method. Statistically significant differences are indicated by different letters ($p < 0.05$).

(C) Chitin-induced marker gene expression in wild-type plants and disruptants. 6-day-old gemmalings were treated with mock (water) or 1 μM GN7 for 1 h; Mp*LRR-RLK*: Mp2g23700.1, Mp*RBOH2*: Mp3g20340.1, Mp*WRKY3*: Mp5g05560.1, Mp*PAL1*: Mp7g14880.1, and Mp*chitinase*: Mp4g20440.1. Data are shown as the mean ± SE. Statistical analysis was performed using Student's t test with p values adjusted by the BH method. Statistically significant differences are indicated by different letters ($p < 0.05$).

(D) Quantification of fungal growth in thalli, inoculated with *Fusarium oxysporum* (*Fo*) f. sp. *lycopersici* 4287 (Fol4287). 3-week-old thalli were dip inoculated with *Fo* (5×10^5 spores mL^{-1}). 4 days post-inoculation, fungal biomass was measured by qPCR of *Fo six1* in inoculated thalli. DNA levels were normalized against *M. polymorpha EF1α*. The relative expression levels (relative fungal biomass) compared with *Fo*-inoculated Tak-1 are shown (n = 4). Statistical analysis was performed using Student's t test with p values adjusted by the BH method. Statistically significant differences are indicated by different letters ($p < 0.05$).

(E and F) Quantification of bacterial growth in the basal region of thalli, inoculated with the bioluminescent *Pto*-lux (n = 8). dpi, days post-inoculation. Boxes show upper and lower quartiles of the value, and lines in boxes represent the medians. Statistical analysis was performed using Student's t test with p values adjusted by the BH method. Statistically significant differences are indicated by different letters ($p < 0.05$).

See also Figures S5 and S6.

Please cite this article in press as: Yotsui et al., LysM-mediated signaling in *Marchantia polymorpha* highlights the conservation of pattern-triggered immunity in land plants, Current Biology (2023), https://doi.org/10.1016/j.cub.2023.07.068

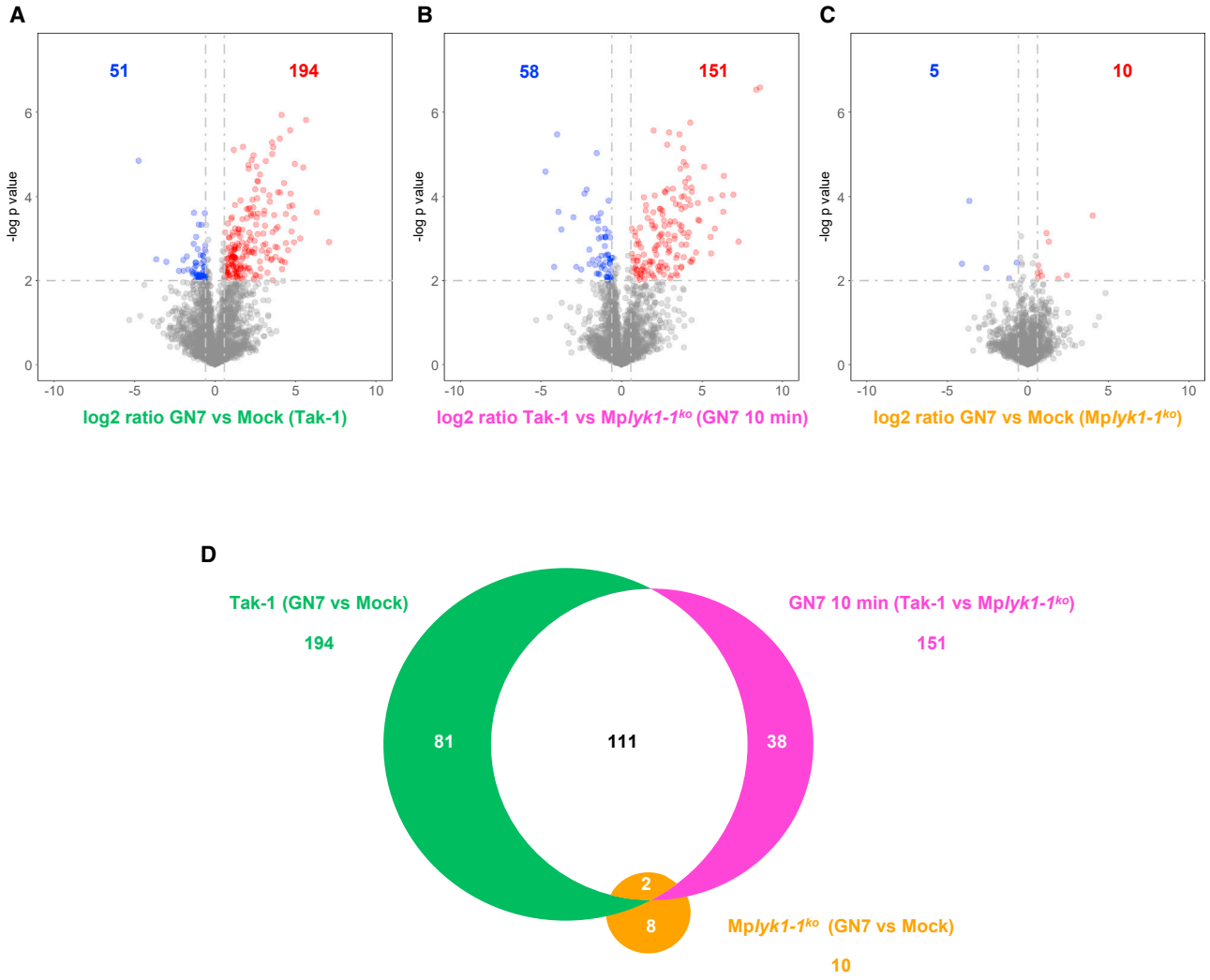

Figure 5. Observed chitin-induced phosphoproteome change mostly depends on MpLYK1

(A–C) Volcano plots showing differential abundance of phosphopeptides between (A) *M. polymorpha* Tak-1 gemmalings treated with mock (water) and 1 μM GN7 for 10 min, (B) *M. polymorpha* Tak-1 and Mp*lyk1-1*^{ko} gemmalings treated with 1 μM GN7 for 10 min, and (C) *M. polymorpha* Mp*lyk1-1*^{ko} gemmalings treated with mock (water) and 1 μM GN7 for 10 min. Each dot represents a single unique phosphopeptide. Significantly increased and decreased phosphopeptides are colored red and blue, respectively ($|\log_2 FC| > 0.58$, $p < 0.01$).

(D) Overlaps of the increased phosphopeptides in (A)–(C).

See also Data S1U–S1Y.

PpCERK is a LYKa-type LysM receptor homolog, which presumably functions as a chitin and PGN receptor or as a co-receptor for signal transduction. However, a contribution of Pp*CERK1* to resistance against pathogenic microbes has not yet been demonstrated. Growth of the liverwort *M. polymorpha* is inhibited by crude extracts from the bacterial and fungal pathogens, *Pto* DC3000, *Plectosphaerella cucumerina*, and *Fo*.[27,28] Crude extracts and chitohexaose treatment can also induce defense-related gene expression in *M. polymorpha*.[28] Note that the analyzed defense-related genes have not been confirmed to be PTI-specific marker genes, and significantly, genetic evidence for the existence of PRRs that sense potential MAMPs is missing in *M. polymorpha*. ROS burst plays an important role during PTI in angiosperms, which can be a good readout for investigating PTI-related components. However, MAMP-induced ROS burst in bryophytes has not yet been reported. Our establishment of a robust ROS burst monitoring method, which utilizes clonal gemmae, and the identification of chitin and PGN fragments as ROS burst-triggering MAMPs will be instrumental in unraveling PTI pathways in the liverwort model *M. polymorpha*. Indeed, using this system we were able to identify MpLYK1 and MpLYR as potential PRRs that are required for sensing chitin and PGN in *M. polymorpha* (Figures 4A, 4B, and S6). In order to establish whether MpLYK1 and/or MpLYR function as genuine MAMP receptors, further biochemical study is required. By characterizing the chitin-induced transcriptional response and through the use of Mp*lyk1*^{ko} and Mp*lyr*^{ge} mutants, we were able to identify PTI-specific marker genes. Our finding that Mp*LYK1* is required for

Please cite this article in press as: Yotsui et al., LysM-mediated signaling in *Marchantia polymorpha* highlights the conservation of pattern-triggered immunity in land plants, Current Biology (2023), https://doi.org/10.1016/j.cub.2023.07.068

CellPress

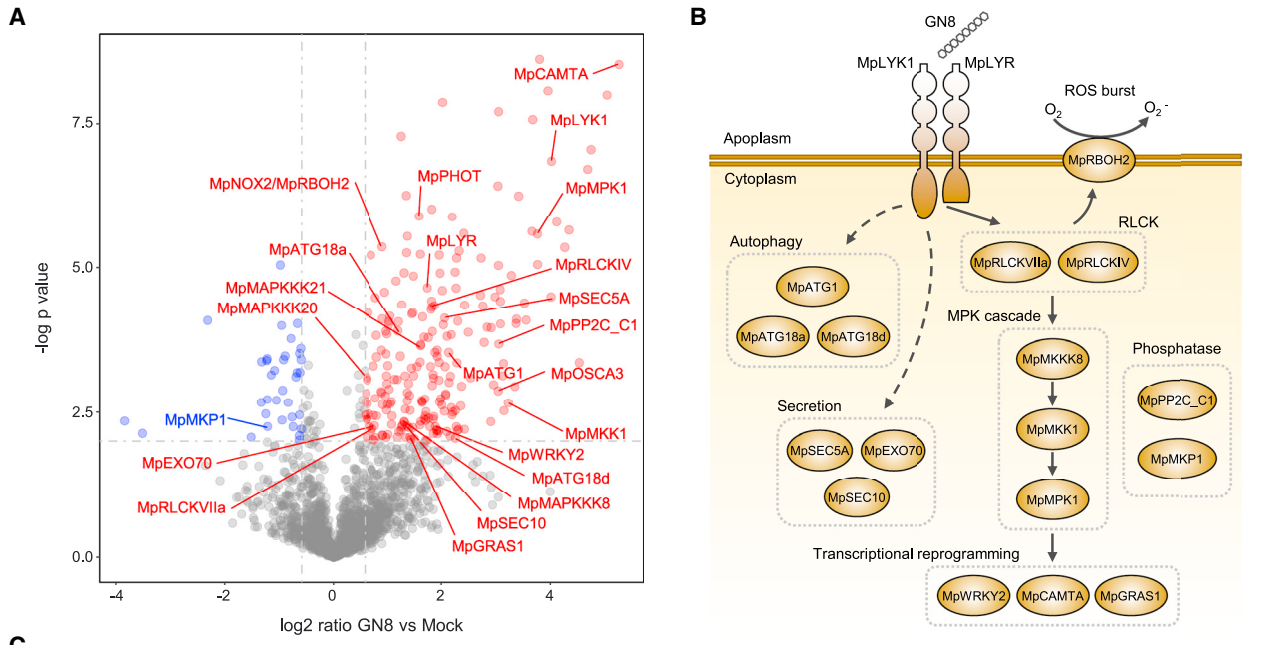

C

LYKa

Juxtamembrane (JM) domain

AaO018.547.1	245	VVAGLCSVIAYFVWRRPRQLVPAKSKEQLAPPGFRASTDPSVSGSSERPLTSGSL–SRTTFSGSYPAADF		313
Sm31503	257	VLLAAAAGMAFFLWKRKHLQQDEKNDRLPSPAASSTVSALRKASGVLRSNISSTT–SVRSAISDIALEKS		325
Sm443457	243	VLAAAVSLVWFFMRRSKKKKVAKYPMDMEVTSADTKHGLLHSPSVGSVPAGLSGFAVDKSVEFTYDELSA		312
AtCERK1	246	LLL––ILFIVYYAYRKNKSKGD––––––SFSSSIPLSTKADHASSTSLQSG–GLGGAGVSPGIAAISVDK		306
MpLYK1	260	LVLAVVLFFLFCVYWPRQRHSDPSNKAAMESLRLDGSQSGDRRSALLKFSQEGAGHSRSSTGSGIPVGPI		329

LYR

Juxtamembrane (JM) domain

AaO050.625.1	291	LVVVGVLGVLWVLRTRRRKEV––––––––––––GGKYDGDFESLPSARSQATGGSDGKSGLA–GDVLLAM		347
Sm11327	297	LLVVLAL––VIFYRRRPRKVTKASLQKSSYGHGGSKDDRNFGAFGSSVSSSYAEPSKEQPSPHAPLLAGM		364
MpLYR	278	VIAAAICAYLVIARKRRRTRTSHGKNSTPLAAISARTDTTSPPYSSDLTPRQQQRLATQGDP––––LEGM		343
AtLYK5	291	LLLSILA––LCFYKRRSKKKS––––––––LPSSLPEENKLFDSSTKQSIPTTTTTQWSIDLSNSSEAFGL		350
AtLYK4	285	VLSVIGAAIFCLSKKKTKTQT––––––––––––––QEETGNLDSFMGKKPPMSDQEFDPLD––––––––GL		333

Kinase domain

AaO050.625.1	432	LVYEFAENGSLADCLRRHVPAAQRGDG––––––GHEGSSAAFLSWNSRLQIALDVATGLEYIHEYINPPF		495
Sm11327	448	LVYEYADNGSLSSCLHNRTPAATAMSKIENAPMGSASVSSAFLSWNTRLQVAMDVATGLEYIHDYTKPSF		517
MpLYR	427	LVYEYAENGSLSDCLHTDFLSKNKM––––––––––ATKSSSFLGWTVRLQIALDVATGLEYIHDYIKPNY		486
AtLYK5	432	LVFEYSENGSISDWLH––––––––––––––––SSGKKSLTWKQRVEIARDVAEALDYLHNYITPPH		481
AtLYK4	415	LVYEHASNGSLSEWIH––––––––––––––––TTKSLLSLTQKLQIALDIATGLNYLHNFADPPY		463

RLCK VII

RLCK VIIc	AtPBL27	54	ELTAPKEGPTA–HIAAQTFT	72
	Sm99936	48	KKEGSRGDES––KIAAQTFT	65
	AaO077.300.1	56	RDPSIKDGSTS–HIAAQTFA	74
	MpRLCKVIIb	73	KEVPTADGAT––HIAAQTFT	90
RLCK VIIb	AtPBL19	56	SPRSIKDLYTEREQNLRVFS	75
RLCK VIIa	AtBIK1	39	AQKTEGEILSST––PVKSFT	56
	Sm151233	59	RSGDEILRQSSG––––LRVFS	75
	AaO018.457.1	33	RLPPPTANPS–––NNLRVFS	49
	MpRLCKVIIa	61	RIALPTVDDSVRGQHLRVFT	80

RBOH

S/T xx L

AtRBOHD	32	ASDRGAFSGPLGRPKRASKK	51
Sm97417	27	GGGAHIATVPLRWDQALDHS	46
AaO006.775.1	29	GSSSTNNSGQLHWQLPDAMA	48
MpRBOH2	23	LKGKPAFSGELNSSGEPAEP	42

S/T xx L

AtRBOHD	337	GDSRILSQM–LSQKLRPAKE	355
Sm97417	299	GYSRDLQQLNYSQTLVAPRR	318
AaO006.775.1	369	GLGRE–AVLQYSQTLVPQRQ	387
MpRBOH2	396	GFSRD–AYLQYSQSLAPQRN	414

D

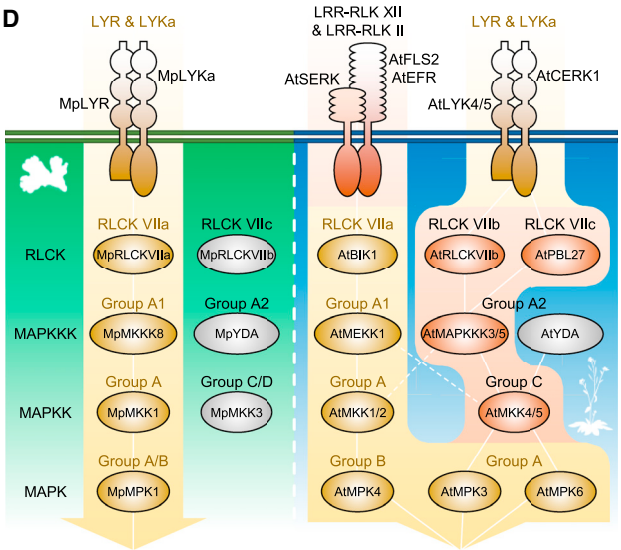

(legend on next page)

Please cite this article in press as: Yotsui et al., LysM-mediated signaling in *Marchantia polymorpha* highlights the conservation of pattern-triggered immunity in land plants, Current Biology (2023), https://doi.org/10.1016/j.cub.2023.07.068

resistance against infection by the bacterial pathogen *Pto* DC3000 and the fungal pathogen Fol4287 could be the first evidence demonstrating the significance of PTI in bryophytes (Figure 4D–4F). As the Mp*lyr*^{ge} mutant did not display hyper-susceptibility to *Pto* DC3000 (Figure 4E), there might be other PRRs that can detect bacterial MAMPs and function together with MpLYK1.

Well-studied PRRs such as *A. thaliana* FLS2 and EFR, which recognize flg22 and elf18, respectively, are LRR-RLKs from subfamily XII (LRR-RLK-XIIs). Genome analysis of *M. polymorpha* and a recent study on the expansion of immune receptor gene repertoires in plants revealed that LRR-RLK-XII genes have undergone expansion within each plant species but with no apparent FLS2 and EFR homologs in many species, including *M. polymorpha*.[35] Therefore, it is not surprising that flg22 and elf18 did not induce ROS burst in *M. polymorpha* (Figure 1A). It would be interesting to investigate whether LRR-RLK-XIIs in *M. polymorpha* also function as PRRs by sensing unidentified MAMPs.

In contrast to LRR-RLK-XIIs, LysM receptors are found to be rather well conserved across entire land plant lineages. Our phylogenetic analysis, based on ectodomain of LysM receptor homologs, indicated that LysM receptors of land plants can be classified into four subgroups (Figures 2A and S3A). The liverwort *M. polymorpha* and the hornworts *Anthoceros agrestis* and *Anthoceros punctatus* have a single gene in each subgroup. LysM receptor homologs of Charophyceae, *Chara braunii* and *Nitella mirabilis*, form an independent subgroup (Figures 2A and S3A). This implies that the last common ancestor of land plants was equipped with a LysM receptor, which might have originated from a streptophyte algae LysM receptor, and suggests that the ancestral LysM receptor was duplicated and sub-functionalized early after terrestrialization and before the emergence of the diversified land plant lineages. Based on studies in angiosperms and considering that LYR-type receptors presumably lack kinase activity, LYRs, including MpLYR, may generally contribute to ligand perception. Concomitantly, LYKa may generally function as a co-receptor for intracellular signal transduction. In *A. thaliana* and rice, several LYPs function as PGN receptors,[12,16] whereas in *M. polymorpha*, we found that MpLYP is not required for PGN-induced ROS burst (Figure 4B and S6). Along the same lines, *P. patens* has lost *LYP* but is able to sense PGN. In different plant lineages, LYPs have sub-functionalized to gain or lose PGN-binding ability. Other LYPs, i.e., OsCEBiP and AtLYM2, function as chitin receptors.[14,36] AtLYM2 does not play a role in conventional PTI responses but regulates chitin-induced plasmodesmata (PD) closure.[36] Expression of Mp*LYP* in storage cells may suggest that MpLYP plays a distinct role, compared with MpLYKs and MpLYR. It would be interesting to investigate whether MpLYP plays a role in PD regulation as AtLYM2. LYKb-type receptors seem to have undergone less expansion but have been retained in most plant species except for mosses. With the exception of a few studies that have described roles of AtLYK3 in the crosstalk between immunity and responses induced by Nod factors or abscisic acid, the molecular functions of LYKb are less understood.[37,38] Further characterization of MpLYK2 may help to uncover the fundamental role of LYKb in plants.

LysM receptors also play a key role in symbiosis establishment. It is thought that the last common ancestor of land plants could establish mutualism with AM fungi.[39] Although *M. polymorpha* is a non-mycorrhizal plant, liverworts in Marchantiales including *Marchantia paleacea* can accommodate AM fungi.[40] Smooth rhizoids of liverworts were shown to be an entry point of AM fungi.[41] We found that Mp*LYK* genes are also expressed in the smooth rhizoids and rhizoid precursor cells (Figure 3). This observation suggests a potential role of LysM receptors in AM symbiosis in Marchantiales. Analysis of LysM receptor homologs in *Marchantia paleacea* would resolve this possibility.

Our phosphoproteome analysis identified several proteins that putatively function downstream of MpLYK1 (Figure 6). We found that the juxtamembrane (JM) domains of MpLYK1 and MpLYR are phospho-regulated upon chitin treatment. The JM domain of AtCERK1 plays a significant role in chitin signal transduction and was shown to be phosphorylated, although the JM domain is generally less conserved at the amino acid sequence level.[32,42] The phospho-regulation of LysM receptor JM domain could be widely conserved regardless of the low sequence conservation. The RBOH is responsible for ROS burst during PTI in plants. In *A. thaliana*, flg22 and elf18 treatment activates AtBIK1, which is a subfamily VIIa RLCK (Figure S3B), to phosphorylate the N-terminal region of AtRBOHD, whose phosphorylation is required for MAMP-induced ROS burst.[33] AtBIK1 preferentially phosphorylates the [S/T]xxL motif.[33] We identified two serine residues in the N-terminal region of MpRBOH2 that were phosphorylated in the chitin-treated condition (Figure 6C). We found that these two phospho-sites correspond to the phospho-sites in AtRBOHD targeted by AtBIK1. These results suggest that MpRBOH2 is responsible for chitin-induced ROS burst and that the AtBIK1 homolog functions downstream of MpLYK1 to activate MpRBOH2. Consistently, we found the only subfamily VIIa RLCK in *M. polymorpha*, MpRLCKVIIa, to be phospho-regulated upon chitin treatment. In *A. thaliana*, RLCKs that belong to the subfamily VIIb and VIIc, but not VIIa, function downstream of

Figure 6. Chitin-induced phosphoproteome changes in *M. polymorpha*

(A) Volcano plots showing differential abundance of phosphopeptides between *M. polymorpha* gemmalings treated with mock (water) and 1 μg/mL GN8. Each dot represents a single unique phosphopeptide. Significantly increased and decreased phosphopeptides are colored red and blue, respectively ($|\log_2 FC| > 0.58$, $p < 0.01$). See Data S1D–S1G.

(B) Predicted chitin-induced signaling pathway in *M. polymorpha* based on the identified phospho-regulated proteins.

(C) Conservation and diversification of the identified phospho-sites. Identified phosphopeptides are marked with red box. Predicted phospho-sites are colored red. Confidently localized phospho-sites are further underlined. Phospho-site information on AtCERK1 is based on Suzuki et al.[32] Serine residues colored green in AtRBOHD are targets of AtBIK1 reported in Kadota et al.[33] At, *Arabidopsis thaliana*; Sm, *Selaginella moellendorffii*; AaO, *Anthoceros agrestis* (Oxford); Mp, *Marchantia polymorpha*.

(D) Schematic representation of PRR signaling pathways in *M. polymorpha* and *A. thaliana*.

See also Figure S3.

Please cite this article in press as: Yotsui et al., LysM-mediated signaling in *Marchantia polymorpha* highlights the conservation of pattern-triggered immunity in land plants, Current Biology (2023), https://doi.org/10.1016/j.cub.2023.07.068

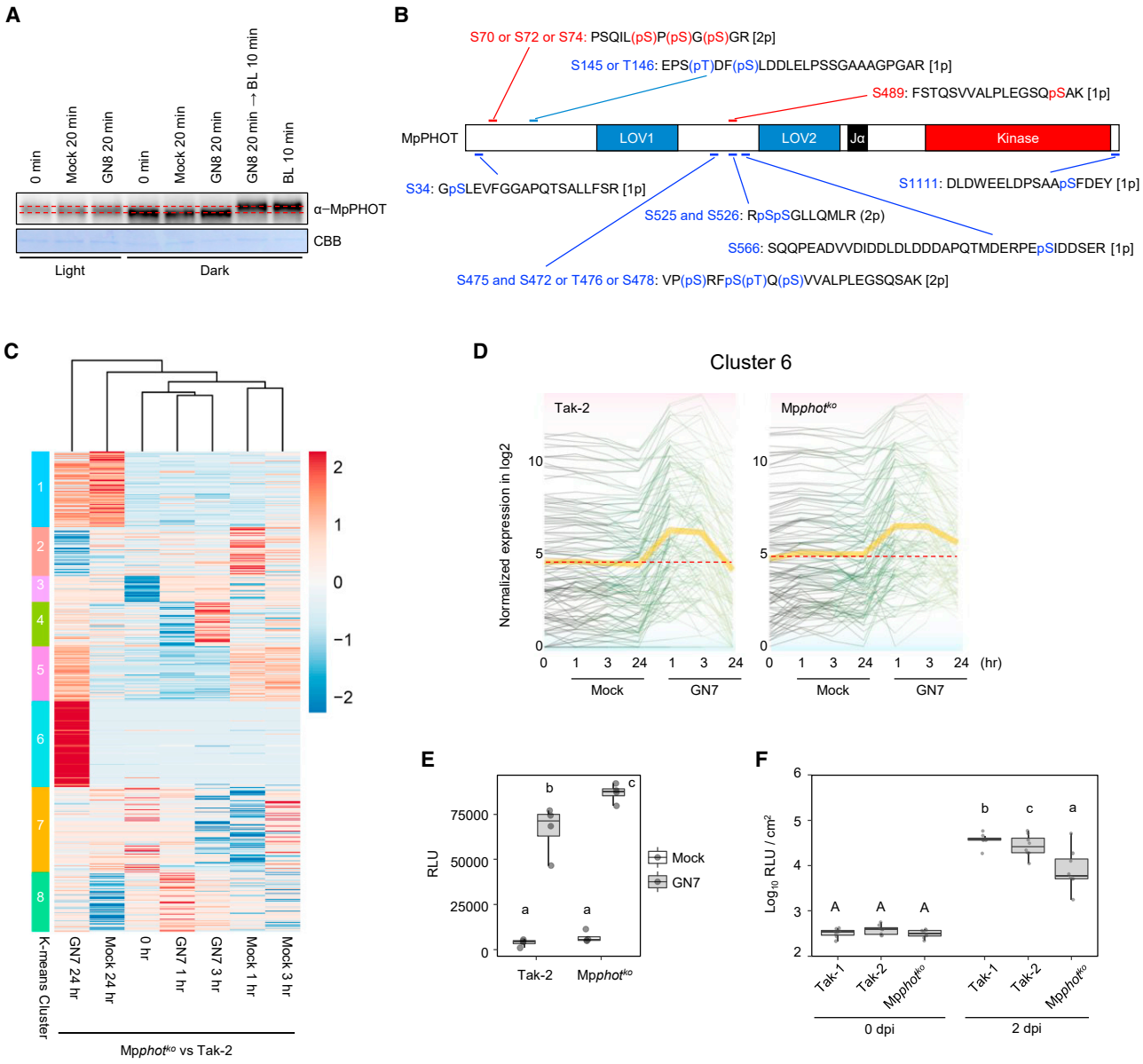

Figure 7. MpPHOT plays a role in PTI in *M. polymorpha*

(A) Western blot analysis of MpPHOT upon mock (water) treatment, 1 μg/mL GN8 treatment, or blue-light (BL) irradiation under the light or dark condition.

(B) Phosphopeptides from MpPHOT induced upon GN8 treatment or blue-light irradiation identified by phosphoproteomics. Phosphopeptides induced by GN8 treatment and blue-light irradiation are colored red and blue, respectively. See Data S1D–S1L.

(C) Clusters of *M. polymorpha* DEGs. Significantly differentially expressed genes showing over ±1 $\log_2$ fold change were grouped based on K-means clustering. Cluster IDs are shown on the left bar. The read count of genes was normalized into the range of ±2. See Data S1S and S1T.

(D) The transcription dynamics of the genes from the K-means cluster 6 (C) showing higher expression trends in GN7-treated condition. Yellow lines indicate mean values.

(E) Chitin-induced ROS burst in Mp*phot*^{ko}. 6-day-old gemmalings were treated with mock (water) or 1 μM GN7. The boxplot indicates total value of RLU measured by luminometer for 30 min after treatments. Boxes show upper and lower quartiles of the value, and black lines represent the medians. Statistical analysis was performed using Student's t test with p values adjusted by the Benjamini-Hochberg (BH) method. Statistically significant differences are indicated by different letters ($p < 0.05$).

(F) Quantification of bacterial growth in the basal region of thallus, inoculated with the bioluminescent *Pto*-lux (n = 8). dpi, days post-inoculation. Boxes show upper and lower quartiles of the value, and black lines represent the medians. Statistical analysis was performed using Student's t test with p values adjusted by the Benjamini-Hochberg (BH) method. Statistically significant differences are indicated by different letters ($p < 0.05$).

See also Figure S7.

AtCERK1.[43,44] However, phospho-regulation of the two remaining RLCK VIIs in *M. polymorpha* was not detected in our analysis. These results suggest that MpRLCKVIIa is responsible for MpLYK1-dependent signaling, although further genetic analysis is needed to confirm this idea. We find it intriguing that RLCK VIIa, group A1 MAPKKK, and group A MAPKK, which function downstream of LRR-RLK-type PRRs *in A. thaliana*, presumably function downstream of LysM-type PRRs in *M. polymorpha* (Figure 6D). Given that the subfamily XII LRR-RLK receptors, which may not function as PRRs in bryophytes, are less conserved in plants, it is possible that LRR-RLK-type PRRs were a tracheophyte innovation and utilized existing PTI signaling components. Considerable expansion of PRR repertoires and downstream kinases and the establishment of complex body plans may have led LysM-type PRRs to utilize other signaling components. It is also possible that *M. polymorpha* has lost signaling components and has uniquely evolved to have a very simple PTI pathway.

Phototropins function as blue-light receptors in tracheophytes as well as in bryophytes and regulate a wide range of blue-light responses.[34,45,46] Recently, potato phototropins, StPHOT1 and StPHOT2, were shown to promote *Phytophthora infestans* infection in *Nicotiana benthamiana*.[47] Conversely, virus-induced silencing of *N. benthamiana* phototropin genes reduced *P. infestans* colonization in *N. benthamiana*.[47] This suggests that phototropin negatively regulates defense against oomycete pathogens in Solanaceae. Similarly, in this study, we found that the only phototropin in *M. polymorpha*, MpPHOT, negatively regulates defense against the bacterial pathogen *Pto* DC3000 (Figure 7F). Chitin-induced transcriptional reprogramming was found to be transient both in *M. polymorpha* and *A. thaliana* (Figures 1E and S1A), which is not surprising because a constitutive immune activation is thought to be costly for plants. However, little is still known about the molecular mechanisms of how plants recover from immune activation. We found that chitin-induced early responses were not markedly affected in Mp*phot*^{ko} (Figures 7D and 7E), indicating that Mp*phot*^{ko} is not an autoimmune mutant exhibiting enhanced PTI responses. Instead, we revealed that Mp*phot*^{ko} has a defect in properly switching off defense-related gene expression or eliminating induced defense-related genes at a later time point (Figure 7D). Further study is needed to unravel the molecular mechanisms underlying this intriguing phenomenon and the significance of chitin-induced phosphorylation of MpPHOT. It is also important to investigate whether phototropin-dependent regulation of defense gene expression is generally conserved in other plant species.

In summary, this study demonstrates that LysM-type PRR-dependent PTI is highly conserved in *M. polymorpha* and that *M. polymorpha* is an attractive plant model for investigating PTI in plants. It is our hope that the methods and genetic resources reported here, as well as the transcriptome and phosphoproteome data, will facilitate further dissection of PTI and its evolution.

STAR★METHODS

Detailed methods are provided in the online version of this paper and include the following:

ACKNOWLEDGMENTS

We thank Naoto Shibuya (Meiji University, Japan) for providing N-acetylchitooctaose. We thank Neysan Donnelly (MPIPZ, Germany) for editing the manuscript. This project was supported by the Max Planck Society and was conducted in the framework of MAdLand (http://madland.science, Deutsche Forschungsgemeinschaft [DFG] Priority Programme 2237). H.N. is grateful for funding by the DFG (NA 946/1-1). This work was supported by JSPS KAKENHI grant numbers 24688007 and 15H01247 to H.N.; 22H00364 to K.S.; 22H04723 to M.S.; and 19H05675, 19H05670, and 21H02515 to T.U. It was also supported by Japan Science and Technology Agency "Precursory Research for Embryonic Science and Technology" (JPMJPR22D3), the Takeda Science Foundation, and the Kato Memorial Bioscience Foundation to M.S.; and by the Spanish Ministry for Science, Innovation, and Universities grant RTI2018-094526-J-I00 to S.G.I.

AUTHOR CONTRIBUTIONS

I.Y. and H.N. designed the research. I.Y., S.S.S., H.I., K.M., R.N., and T. Kohchi generated plant materials. T. Kanazawa, K.M., H.-W.J., and T.U. performed microscopic analysis. T.S., S.G.I., and K.M. performed *Pto* DC3000 infection assay. S.M. and S.G.I. performed Fol4287 infection assay. I.Y., Y.I., M.S., K.S., and S.M. performed transcriptomic analysis. I.Y., Y.N., H.M., S.C.S., Y.Y., A.H., and H.N. performed phosphoproteomic analysis. I.Y. performed all other experiments. I.Y., H.M., and H.N. wrote the manuscript. All authors corrected the manuscript.

DECLARATION OF INTERESTS

The authors declare no competing interests.

Received: January 5, 2023
Revised: May 25, 2023
Accepted: July 31, 2023
Published: August 23, 2023

REFERENCES

1. Zipfel, C., and Oldroyd, G.E.D. (2017). Plant signalling in symbiosis and immunity. Nature *543*, 328–336.

2. Boller, T., and Felix, G. (2009). A renaissance of elicitors: perception of microbe-associated molecular patterns and danger signals by pattern-recognition receptors. Annu. Rev. Plant Biol. *60*, 379–406.
3. Chinchilla, D., Bauer, Z., Regenass, M., Boller, T., and Felix, G. (2006). The *Arabidopsis* receptor kinase FLS2 binds flg22 and determines the specificity of flagellin perception. Plant Cell *18*, 465–476.
4. Zipfel, C., Kunze, G., Chinchilla, D., Caniard, A., Jones, J.D.G., Boller, T., and Felix, G. (2006). Perception of the bacterial PAMP EF-Tu by the receptor EFR restricts *Agrobacterium*-mediated transformation. Cell *125*, 749–760.
5. Chinchilla, D., Zipfel, C., Robatzek, S., Kemmerling, B., Nürnberger, T., Jones, J.D.G., Felix, G., and Boller, T. (2007). A flagellin-induced complex of the receptor FLS2 and BAK1 initiates plant defence. Nature *448*, 497–500.
6. Roux, M., Schwessinger, B., Albrecht, C., Chinchilla, D., Jones, A., Holton, N., Malinovsky, F.G., Tör, M., Vries, S. de, and Zipfel, C. (2011). The *Arabidopsis* leucine-rich repeat receptor–like kinases BAK1/SERK3 and BKK1/SERK4 are required for innate immunity to hemibiotrophic and biotrophic pathogens. Plant Cell *23*, 2440–2455.
7. Li, J., Wen, J., Lease, K.A., Doke, J.T., Tax, F.E., and Walker, J.C. (2002). BAK1, an *Arabidopsis* LRR receptor-like protein kinase, interacts with BRI1 and modulates brassinosteroid signaling. Cell *110*, 213–222.
8. Gust, A.A., Willmann, R., Desaki, Y., Grabherr, H.M., and Nürnberger, T. (2012). Plant LysM proteins: modules mediating symbiosis and immunity. Trends Plant Sci. *17*, 495–502.
9. Tanaka, K., Nguyen, C.T., Liang, Y., Cao, Y., and Stacey, G. (2013). Role of LysM receptors in chitin-triggered plant innate immunity. Plant Signal. Behav. *8*, e22598.
10. Miya, A., Albert, P., Shinya, T., Desaki, Y., Ichimura, K., Shirasu, K., Narusaka, Y., Kawakami, N., Kaku, H., and Shibuya, N. (2007). CERK1, a LysM receptor kinase, is essential for chitin elicitor signaling in *Arabidopsis*. Proc. Natl. Acad. Sci. USA *104*, 19613–19618.
11. Cao, Y., Liang, Y., Tanaka, K., Nguyen, C.T., Jedrzejczak, R.P., Joachimiak, A., and Stacey, G. (2014). The kinase LYK5 is a major chitin receptor in *Arabidopsis* and forms a chitin-induced complex with related kinase CERK1. eLife *3*, e03766.
12. Willmann, R., Lajunen, H.M., Erbs, G., Newman, M.A., Kolb, D., Tsuda, K., Katagiri, F., Fliegmann, J., Bono, J.J., Cullimore, J.V., et al. (2011). *Arabidopsis* lysin-motif proteins LYM1 LYM3 CERK1 mediate bacterial peptidoglycan sensing and immunity to bacterial infection. Proc. Natl. Acad. Sci. USA *108*, 19824–19829.
13. Gimenez-Ibanez, S., Hann, D.R., Ntoukakis, V., Petutschnig, E., Lipka, V., and Rathjen, J.P. (2009). AvrPtoB targets the LysM receptor kinase CERK1 to promote bacterial virulence on plants. Curr. Biol. *19*, 423–429.
14. Kaku, H., Nishizawa, Y., Ishii-Minami, N., Akimoto-Tomiyama, C., Dohmae, N., Takio, K., Minami, E., and Shibuya, N. (2006). Plant cells recognize chitin fragments for defense signaling through a plasma membrane receptor. Proc. Natl. Acad. Sci. USA *103*, 11086–11091.
15. Shimizu, T., Nakano, T., Takamizawa, D., Desaki, Y., Ishii-Minami, N., Nishizawa, Y., Minami, E., Okada, K., Yamane, H., Kaku, H., et al. (2010). Two LysM receptor molecules, CEBiP and OsCERK1, cooperatively regulate chitin elicitor signaling in rice. Plant J. *64*, 204–214.
16. Liu, B., Li, J.F., Ao, Y., Qu, J., Li, Z., Su, J., Zhang, Y., Liu, J., Feng, D., Qi, K., et al. (2012). Lysin motif–containing proteins LYP4 and LYP6 play dual roles in peptidoglycan and chitin perception in rice innate immunity. Plant Cell *24*, 3406–3419.
17. Bozsoki, Z., Gysel, K., Hansen, S.B., Lironi, D., Krönauer, C., Feng, F., Jong, N. de, Vinther, M., Kamble, M., Thygesen, M.B., et al. (2020). Ligand-recognizing motifs in plant LysM receptors are major determinants of specificity. Science *369*, 663–670.
18. Miyata, K., Kozaki, T., Kouzai, Y., Ozawa, K., Ishii, K., Asamizu, E., Okabe, Y., Umehara, Y., Miyamoto, A., Kobae, Y., et al. (2014). The bifunctional plant receptor, OsCERK1, regulates both chitin-triggered immunity and arbuscular mycorrhizal symbiosis in rice. Plant Cell Physiol. *55*, 1864–1872.
19. Zhang, X., Dong, W., Sun, J., Feng, F., Deng, Y., He, Z., Oldroyd, G.E.D., and Wang, E. (2015). The receptor kinase *CERK1* has dual functions in symbiosis and immunity signalling. Plant J. *81*, 258–267.
20. Carotenuto, G., Chabaud, M., Miyata, K., Capozzi, M., Takeda, N., Kaku, H., Shibuya, N., Nakagawa, T., Barker, D.G., and Genre, A. (2017). The rice LysM receptor-like kinase OsCERK1 is required for the perception of short-chain chitin oligomers in arbuscular mycorrhizal signaling. New Phytol. *214*, 1440–1446.
21. Rensing, S.A., Lang, D., Zimmer, A.D., Terry, A., Salamov, A., Shapiro, H., Nishiyama, T., Perroud, P.F., Lindquist, E.A., Kamisugi, Y., et al. (2008). The *Physcomitrella* genome reveals evolutionary insights into the conquest of land by plants. Science *319*, 64–69.
22. Bowman, J.L., Kohchi, T., Yamato, K.T., Jenkins, J., Shu, S., Ishizaki, K., Yamaoka, S., Nishihama, R., Nakamura, Y., Berger, F., et al. (2017). Insights into land plant evolution garnered from the *Marchantia polymorpha* genome. Cell *171*, 287–304.e15.
23. Zhang, J., Fu, X.X., Li, R.Q., Zhao, X., Liu, Y., Li, M.H., Zwaenepoel, A., Ma, H., Goffinet, B., Guan, Y.L., et al. (2020). The hornwort genome and early land plant evolution. Nat. Plants *6*, 107–118.
24. Li, F.W., Nishiyama, T., Waller, M., Frangedakis, E., Keller, J., Li, Z., Fernandez-Pozo, N., Barker, M.S., Bennett, T., Blázquez, M.A., et al. (2020). *Anthoceros* genomes illuminate the origin of land plants and the unique biology of hornworts. Nat. Plants *6*, 259–272.
25. Nishiyama, T., Sakayama, H., Vries, J. de, Buschmann, H., Saint-Marcoux, D., Ullrich, K.K., Haas, F.B., Vanderstraeten, L., Becker, D., Lang, D., et al. (2018). The *Chara* genome: secondary complexity and implications for plant terrestrialization. Cell *174*, 448–464.e24.
26. Bressendorff, S., Azevedo, R., Kenchappa, C.S., Ponce de León, I.P. de, Olsen, J.V., Rasmussen, M.W., Erbs, G., Newman, M.A., Petersen, M., and Mundy, J. (2016). An innate immunity pathway in the moss *Physcomitrella patens*. Plant Cell *28*, 1328–1342.
27. Gimenez-Ibanez, S., Zamarreño, A.M., García-Mina, J.M., and Solano, R. (2019). An evolutionarily ancient immune system governs the interactions between *Pseudomonas syringae* and an early-diverging land plant lineage. Curr. Biol. *29*, 2270–2281.e4.
28. Redkar, A., Gimenez Ibanez, S., Sabale, M., Zechmann, B., Solano, R., and Di Pietro, A. (2022). *Marchantia polymorpha* model reveals conserved infection mechanisms in the vascular wilt fungal pathogen *Fusarium oxysporum*. New Phytol. *234*, 227–241.
29. Carella, P., Gogleva, A., Tomaselli, M., Alfs, C., and Schornack, S. (2018). *Phytophthora palmivora* establishes tissue-specific intracellular infection structures in the earliest divergent land plant lineage. Proc. Natl. Acad. Sci. USA *115*, E3846–E3855.
30. Iwakawa, H., Melkonian, K., Schlüter, T., Jeon, H.W., Nishihama, R., Motose, H., and Nakagami, H. (2021). *Agrobacterium*-mediated transient transformation of *Marchantia* liverworts. Plant Cell Physiol. *62*, 1718–1727.
31. Shimamura, M. (2016). *Marchantia polymorpha*: taxonomy, phylogeny and morphology of a model system. Plant Cell Physiol. *57*, 230–256.
32. Suzuki, M., Yoshida, I., Suto, K., Desaki, Y., Shibuya, N., and Kaku, H. (2019). AtCERK1 phosphorylation site S493 contributes to the transphosphorylation of downstream components for chitin-induced immune signaling. Plant Cell Physiol. *60*, 1804–1810.
33. Kadota, Y., Sklenar, J., Derbyshire, P., Stransfeld, L., Asai, S., Ntoukakis, V., Jones, J.D., Shirasu, K., Menke, F., Jones, A., et al. (2014). Direct regulation of the NADPH oxidase RBOHD by the PRR-associated kinase BIK1 during plant immunity. Mol. Cell *54*, 43–55.
34. Komatsu, A., Terai, M., Ishizaki, K., Suetsugu, N., Tsuboi, H., Nishihama, R., Yamato, K.T., Wada, M., and Kohchi, T. (2014). Phototropin encoded by a single-copy gene mediates chloroplast photorelocation movements in the liverwort *Marchantia polymorpha*. Plant Physiol. *166*, 411–427.

35. Ngou, B.P.M., Heal, R., Wyler, M., Schmid, M.W., and Jones, J.D.G. (2022). Concerted expansion and contraction of immune receptor gene repertoires in plant genomes. Nat. Plants *8*, 1146–1152.

36. Faulkner, C., Petutschnig, E., Benitez-Alfonso, Y., Beck, M., Robatzek, S., Lipka, V., and Maule, A.J. (2013). LYM2-dependent chitin perception limits molecular flux via plasmodesmata. Proc. Natl. Acad. Sci. USA *110*, 9166–9170.

37. Liang, Y., Cao, Y., Tanaka, K., Thibivilliers, S., Wan, J., Choi, J., Kang, C.h., Qiu, J., and Stacey, G. (2013). Nonlegumes respond to rhizobial Nod factors by suppressing the innate immune response. Science *341*, 1384–1387.

38. Paparella, C., Savatin, D.V., Marti, L., De Lorenzo, G.D., and Ferrari, S. (2014). The Arabidopsis LYSIN MOTIF-CONTAINING RECEPTOR-LIKE KINASE3 regulates the cross talk between immunity and abscisic acid responses. Plant Physiol. *165*, 262–276.

39. Rich, M.K., Vigneron, N., Libourel, C., Keller, J., Xue, L., Hajheidari, M., Radhakrishnan, G.V., Le Ru, A.L., Diop, S.I., Potente, G., et al. (2021). Lipid exchanges drove the evolution of mutualism during plant terrestrialization. Science *372*, 864–868.

40. Humphreys, C.P., Franks, P.J., Rees, M., Bidartondo, M.I., Leake, J.R., and Beerling, D.J. (2010). Mutualistic mycorrhiza-like symbiosis in the most ancient group of land plants. Nat. Commun. *1*, 103.

41. Russell, J., and Bulman, S. (2005). The liverwort *Marchantia foliacea* forms a specialized symbiosis with arbuscular mycorrhizal fungi in the genus Glomus. New Phytol. *165*, 567–579.

42. Zhou, Q., Liu, J., Wang, J., Chen, S., Chen, L., Wang, J., Wang, H.B., and Liu, B. (2020). The juxtamembrane domains of Arabidopsis CERK1, BAK1, and FLS2 play a conserved role in chitin-induced signaling. J. Integr. Plant Biol. *62*, 556–562.

43. Yamada, K., Yamaguchi, K., Shirakawa, T., Nakagami, H., Mine, A., Ishikawa, K., Fujiwara, M., Narusaka, M., Narusaka, Y., Ichimura, K., et al. (2016). The *Arabidopsis* CERK1-associated kinase PBL27 connects chitin perception to MAPK activation. EMBO J. *35*, 2468–2483.

44. Bi, G., Zhou, Z., Wang, W., Li, L., Rao, S., Wu, Y., Zhang, X., Menke, F.L.H., Chen, S., and Zhou, J.-M. (2018). Receptor-like cytoplasmic kinases directly link diverse pattern recognition receptors to the activation of mitogen-activated protein kinase cascades in Arabidopsis. Plant Cell *30*, 1543–1561.

45. Kasahara, M., Kagawa, T., Sato, Y., Kiyosue, T., and Wada, M. (2004). Phototropins mediate blue and red light-induced chloroplast movements in *Physcomitrella patens*. Plant Physiol. *135*, 1388–1397.

46. Christie, J.M. (2007). Phototropin blue-light receptors. Annu. Rev. Plant Biol. *58*, 21–45.

47. Naqvi, S., He, Q., Trusch, F., Qiu, H., Pham, J., Sun, Q., Christie, J.M., Gilroy, E.M., and Birch, P.R.J. (2022). Blue-light receptor phototropin 1 suppresses immunity to promote *Phytophthora infestans* infection. New Phytol. *233*, 2282–2293.

48. Matsumoto, A., Schlüter, T., Melkonian, K., Takeda, A., Nakagami, H., and Mine, A. (2022). A versatile Tn7 transposon-based bioluminescence tagging tool for quantitative and spatial detection of bacteria in plants. Plant Commun. *3*, 100227.

49. Ishizaki, K., Johzuka-Hisatomi, Y., Ishida, S., Iida, S., and Kohchi, T. (2013). Homologous recombination-mediated gene targeting in the liverwort *Marchantia polymorpha* L. Sci. Rep. *3*, 1532.

50. Sugano, S.S., Nishihama, R., Shirakawa, M., Takagi, J., Matsuda, Y., Ishida, S., Shimada, T., Hara-Nishimura, I., Osakabe, K., and Kohchi, T. (2018). Efficient CRISPR/Cas9-based genome editing and its application to conditional genetic analysis in *Marchantia polymorpha*. PLoS One *13*, e0205117.

51. Ishizaki, K., Nishihama, R., Ueda, M., Inoue, K., Ishida, S., Nishimura, Y., Shikanai, T., and Kohchi, T. (2015). Development of gateway binary vector series with four different selection markers for the liverwort *Marchantia polymorpha*. PLoS One *10*, e0138876.

52. Kumar, R., Ichihashi, Y., Kimura, S., Chitwood, D.H., Headland, L.R., Peng, J., Maloof, J.N., and Sinha, N.R. (2012). A high-throughput method for Illumina RNA-seq library preparation. Front. Plant Sci. *3*, 202.

53. Kanehisa, M., Sato, Y., and Morishima, K. (2016). BlastKOALA and GhostKOALA: KEGG tools for functional characterization of genome and metagenome sequences. J. Mol. Biol. *428*, 726–731.

54. Lombard, V., Golaconda Ramulu, H.G., Drula, E., Coutinho, P.M., and Henrissat, B. (2014). The carbohydrate-active enzymes database (CAZy) in 2013. Nucleic Acids Res. *42*, D490–D495.

55. Gene Ontology Consortium (2015). Gene Ontology Consortium: going forward. Nucleic Acids Res. *43*, D1049–D1056.

56. Ogata, H., Goto, S., Sato, K., Fujibuchi, W., Bono, H., and Kanehisa, M. (1999). KEGG: Kyoto encyclopedia of genes and genomes. Nucleic Acids Res. *27*, 29–34.

57. Tatusov, R.L., Fedorova, N.D., Jackson, J.D., Jacobs, A.R., Kiryutin, B., Koonin, E.V., Krylov, D.M., Mazumder, R., Mekhedov, S.L., Nikolskaya, A.N., et al. (2003). The COG database: an updated version includes eukaryotes. BMC Bioinform. *4*, 41.

58. Finn, R.D., Coggill, P., Eberhardt, R.Y., Eddy, S.R., Mistry, J., Mitchell, A.L., Potter, S.C., Punta, M., Qureshi, M., Sangrador-Vegas, A., et al. (2016). The Pfam protein families database: towards a more sustainable future. Nucleic Acids Res. *44*, D279–D285.

59. Thomas, P.D., Campbell, M.J., Kejariwal, A., Mi, H., Karlak, B., Daverman, R., Diemer, K., Muruganujan, A., and Narechania, A. (2003). PANTHER: a library of protein families and subfamilies indexed by function. Genome Res. *13*, 2129–2141.

60. Rawlings, N.D., Barrett, A.J., Thomas, P.D., Huang, X., Bateman, A., and Finn, R.D. (2018). The *MEROPS* database of proteolytic enzymes, their substrates and inhibitors in 2017 and a comparison with peptidases in the PANTHER database. Nucleic Acids Res. *46*, D624–D632.

61. Carlson, M. (2016). KEGG.db: a set of annotation maps for KEGG. R package, version 3.2.3. https://bioconductor.riken.jp/packages/3.10/data/annotation/html/KEGG.db.html.

62. Carlson, M. (2019). GO.db: a set of annotation maps describing the entire gene ontology. R package version 3.8.2. https://bioconductor.org/packages/release/data/annotation/html/GO.db.html.

63. Carlson, M., Liu, T.-Y., Lin, C., Falcon, S., Zhang, J., and MacDonald, J.W. (2019). PFAM.db: a set of protein ID mappings for PFAM. R package version 3.8.2. https://bioconductor.org/packages/release/data/annotation/html/PFAM.db.html.

64. Chen, S., Zhou, Y., Chen, Y., and Gu, J. (2018). fastp: an ultra-fast all-in-one FASTQ preprocessor. Bioinformatics *34*, i884–i890.

65. Dobin, A., Davis, C.A., Schlesinger, F., Drenkow, J., Zaleski, C., Jha, S., Batut, P., Chaisson, M., and Gingeras, T.R. (2013). STAR: ultrafast universal RNA-seq aligner. Bioinformatics *29*, 15–21.

66. Love, M.I., Huber, W., and Anders, S. (2014). Moderated estimation of fold change and dispersion for RNA-seq data with DESeq2. Genome Biol. *15*, 550.

67. Kolde, R. (2019). pheatmap: pretty heatmaps. R package version 1.0.12. https://rdrr.io/cran/pheatmap/.

68. Miyauchi, S., Navarro, D., Grigoriev, I.V., Lipzen, A., Riley, R., Chevret, D., Grisel, S., Berrin, J.G., Henrissat, B., and Rosso, M.N. (2016). Visual comparative omics of fungi for plant biomass deconstruction. Front. Microbiol. *7*, 1335.

69. Miyauchi, S., Navarro, D., Grisel, S., Chevret, D., Berrin, J.G., and Rosso, M.N. (2017). The integrative omics of white-rot fungus *Pycnoporus coccineus* reveals co-regulated CAZymes for orchestrated lignocellulose breakdown. PLoS One *12*, e0175528.

70. Miyauchi, S., Rancon, A., Drula, E., Hage, H., Chaduli, D., Favel, A., Grisel, S., Henrissat, B., Herpoël-Gimbert, I., Ruiz-Dueñas, F.J., et al. (2018). Integrative visual omics of the white-rot fungus *Polyporus brumalis* exposes the biotechnological potential of its oxidative enzymes for delignifying raw plant biomass. Biotechnol. Biofuels *11*, 201.

71. Miyauchi, S., Hage, H., Drula, E., Lesage-Meessen, L., Berrin, J.G., Navarro, D., Favel, A., Chaduli, D., Grisel, S., Haon, M., et al. (2020). Conserved white-rot enzymatic mechanism for wood decay in the Basidiomycota genus *Pycnoporus*. DNA Res. *27*, 2.

72. R Core Team (2013). A Language and Environment for Statistical Computing (R Foundation for Statistical Computing).

73. Zhou, Y., Zhou, B., Pache, L., Chang, M., Khodabakhshi, A.H., Tanaseichuk, O., Benner, C., and Chanda, S.K. (2019). Metascape provides a biologist-oriented resource for the analysis of systems-level datasets. Nat. Commun. *10*, 1523.

74. Tian, T., Liu, Y., Yan, H., You, Q., Yi, X., Du, Z., Xu, W., and Su, Z. (2017). agriGO v2.0: a GO analysis toolkit for the agricultural community, 2017 update. Nucleic Acids Res. *45*, W122–W129.

75. Edgar, R.C. (2004). MUSCLE: multiple sequence alignment with high accuracy and high throughput. Nucleic Acids Res. *32*, 1792–1797.

76. Guindon, S., and Gascuel, O. (2003). A simple, fast, and accurate algorithm to estimate large phylogenies by maximum likelihood. Syst. Biol. *52*, 696–704.

77. Cox, J., and Mann, M. (2008). MaxQuant enables high peptide identification rates, individualized p.p.b.-range mass accuracies and proteome-wide protein quantification. Nat. Biotechnol. *26*, 1367–1372.

78. Tyanova, S., Temu, T., Sinitcyn, P., Carlson, A., Hein, M.Y., Geiger, T., Mann, M., and Cox, J. (2016). The Perseus computational platform for comprehensive analysis of (prote)omics data. Nat. Methods *13*, 731–740.

79. Sun, G., Xu, Y., Liu, H., Sun, T., Zhang, J., Hettenhausen, C., Shen, G., Qi, J., Qin, Y., Li, J., et al. (2018). Large-scale gene losses underlie the genome evolution of parasitic plant *Cuscuta australis*. Nat. Commun. *9*, 2683.

80. Vogel, A., Schwacke, R., Denton, A.K., Usadel, B., Hollmann, J., Fischer, K., Bolger, A., Schmidt, M.H.-W., Bolger, M.E., Gundlach, H., et al. (2018). Footprints of parasitism in the genome of the parasitic flowering plant *Cuscuta campestris*. Nat. Commun. *9*, 2515.

81. Banks, J.A., Nishiyama, T., Hasebe, M., Bowman, J.L., Gribskov, M., dePamphilis, C., Albert, V.A., Aono, N., Aoyama, T., Ambrose, B.A., et al. (2011). The selaginella genome identifies genetic changes associated with the evolution of vascular plants. Science *332*, 960–963.

82. Ju, C., Van de Poel, B.V. de, Cooper, E.D., Thierer, J.H., Gibbons, T.R., Delwiche, C.F., and Chang, C. (2015). Conservation of ethylene as a plant hormone over 450 million years of evolution. Nat. Plants *1*, 14004.

83. Delaux, P.M., Radhakrishnan, G.V., Jayaraman, D., Cheema, J., Malbreil, M., Volkening, J.D., Sekimoto, H., Nishiyama, T., Melkonian, M., Pokorny, L., et al. (2015). Algal ancestor of land plants was preadapted for symbiosis. Proc. Natl. Acad. Sci. USA *112*, 13390–13395.

84. Madsen, E.B., Madsen, L.H., Radutoiu, S., Olbryt, M., Rakwalska, M., Szczyglowski, K., Sato, S., Kaneko, T., Tabata, S., Sandal, N., et al. (2003). A receptor kinase gene of the LysM type is involved in legume perception of rhizobial signals. Nature *425*, 637–640.

85. Kubota, A., Ishizaki, K., Hosaka, M., and Kohchi, T. (2013). Efficient agrobacterium-mediated transformation of the liverwort *Marchantia polymorpha* using regenerating thalli. Biosci. Biotechnol. Biochem. *77*, 167–172.

86. Ishizaki, K., Chiyoda, S., Yamato, K.T., and Kohchi, T. (2008). *Agrobacterium*-mediated transformation of the haploid liverwort *Marchantia polymorpha* L., an emerging model for plant biology. Plant Cell Physiol. *49*, 1084–1091.

87. Sugano, S.S., Shirakawa, M., Takagi, J., Matsuda, Y., Shimada, T., Hara-Nishimura, I., and Kohchi, T. (2014). CRISPR/Cas9-mediated targeted mutagenesis in the liverwort *Marchantia polymorpha* L. Plant Cell Physiol. *55*, 475–481.

88. Jefferson, R.A., Kavanagh, T.A., and Bevan, M.W. (1987). GUS fusions: β-glucuronidase as a sensitive and versatile gene fusion marker in higher plants. EMBO J. *6*, 3901–3907.

89. Ishizaki, K., Nonomura, M., Kato, H., Yamato, K.T., and Kohchi, T. (2012). Visualization of auxin-mediated transcriptional activation using a common auxin-responsive reporter system in the liverwort *Marchantia polymorpha*. J. Plant Res. *125*, 643–651.

90. Koide, E., Suetsugu, N., Iwano, M., Gotoh, E., Nomura, Y., Stolze, S.C., Nakagami, H., Kohchi, T., and Nishihama, R. (2020). Regulation of photosynthetic carbohydrate metabolism by a raf-like kinase in the liverwort *Marchantia polymorpha*. Plant Cell Physiol. *61*, 631–643.

91. Tyanova, S., Temu, T., and Cox, J. (2016). The MaxQuant computational platform for mass spectrometry-based shotgun proteomics. Nat. Protoc. *11*, 2301–2319.

Please cite this article in press as: Yotsui et al., LysM-mediated signaling in *Marchantia polymorpha* highlights the conservation of pattern-triggered immunity in land plants, Current Biology (2023), https://doi.org/10.1016/j.cub.2023.07.068

STAR★METHODS

KEY RESOURCES TABLE

REAGENT or RESOURCE	SOURCE	IDENTIFIER
Antibodies		
Phospho-p44/42 MAPK (Erk1/2)(Thr202/Thr204) (D13.14.4E)XP Rabbit mAb	Cell Signaling	Cat#4370; RRID: AB_2315112
goat anti-rabbit IgG-HRP	SANTA CRUZ BIOTECHNOLOGY, INC.	sc-2004; RRID: AB_631746
α-MpPHOT	Komatsu et al.[34]	N/A
Bacterial and virus strains		
Escherichia coli DH5a	Widely distributed	N/A
Agrobacterium tumefaciens GV2260	Widely distributed	N/A
Fusarium oxysporum (*Fo*) f.sp. *lycopersici* 4287 (Fol4287)	Redkar et al.[28]	N/A
bioluminescent *Pseudomonas syringae* pv. *tomato* DC3000 (*Pto*-lux)	Matsumoto et al.[48]	N/A
Chemicals, peptides, and recombinant proteins		
L-012	TaKaRa	Cat#120-04891
flg22	Eurofins	N/A
elf18	Eurofins	N/A
Lipopolysaccharides from *Pseudomonas aeruginosa* serotype 10	SIGMA	L9143
GN6 (N-acetylchitohexaose)	SEIKAGAKU BIOBUSINESS CORPORATION	Cat#400427
GN7 (N-acetylchitoheptaose)	ELICITYL	GLU437
GN8 (N-acetylchitooctaose)	Naoto Shibuya, Meiji University	N/A
Peptidoglycan from *Bacillus subtilis*	SIGMA	Cat#69554
Peroxidase from horseradish	SIGMA	P8125
ISOPLANT II	NIPPON GENE	Cat#310-04151
RNeasy Plant Mini Kit	QIAGEN	Cat#74904
NucleoSpin RNA Plant	Clontech	Cat#740949.50
ReverTra Ace qPCR RT Master Mix with gDNA Remover	TOYOBO	FSQ-301
KOD-Plus-Neo	TOYOBO	KOD-401
KOD FX Neo	TOYOBO	KFX-201
Quick Taq HS DyeMix	TOYOBO	DTM-101
PrimeSTAR Mutagenesis Basal Kit	TaKaRa	R046A
In-Fusion HD cloning kit	Clontech	Cat#639649
Gateway LR Clonase II Enzyme Mix	ThermoFisher	Cat#11791020
THUNDERBIRD SYBR qPCR Mix	TOYOBO	QPS-201
5-Bromo-4chloro-3-indolyl β-D-glucuronide cyclohexylamine salt (X-gluc)	Rose Scientific Ltd.	ES-1007-001
Deposited data		
RNA-seq data	This study	NCBI BioProject: PRJNA917430
MS proteomics data	This study	ProteomeXchange: PXD038903, PXD038907, and PXD042084
Experimental models: Organisms/strains		
Marchantia polymorpha: Tak-1 (male)	Takayuki Kohchi, Kyoto University	N/A

(*Continued on next page*)

Please cite this article in press as: Yotsui et al., LysM-mediated signaling in *Marchantia polymorpha* highlights the conservation of pattern-triggered immunity in land plants, Current Biology (2023), https://doi.org/10.1016/j.cub.2023.07.068

Continued

REAGENT or RESOURCE	SOURCE	IDENTIFIER
Marchantia polymorpha: Tak-2 (female)	Takayuki Kohchi, Kyoto University	N/A
Marchantia polymorpha: $_{pro}$Mp*LYK1*:*GUS*/Tak-1	This study	N/A
Marchantia polymorpha: $_{pro}$Mp*LYK2*:*GUS*/Tak-1	This study	N/A
Marchantia polymorpha: $_{pro}$Mp*LYR*:*GUS*/Tak-1	This study	N/A
Marchantia polymorpha: $_{pro}$Mp*LYP*:*GUS*/Tak-1	This study	N/A
Marchantia polymorpha: Mp*lyk1-1*^{ko} (male)	This study	N/A
Marchantia polymorpha: Mp*lyk1-2*^{ko} (female)	This study	N/A
Marchantia polymorpha: Mp*lyk2*^{ko} (male)	This study	N/A
Marchantia polymorpha: Mp*lyr-1*^{ge} (female)	This study	N/A
Marchantia polymorpha: Mp*lyr-2*^{ge} (male)	This study	N/A
Marchantia polymorpha: Mp*lyr-3*^{ge} (male)	This study	N/A
Marchantia polymorpha: Mp*lyp*^{ko} (male)	This study	N/A
Marchantia polymorpha: $_{pro}$Mp*LYK1*:Mp*LYK1*$^{\#1}$/Mp*lyk1-1*^{ko}	This study	N/A
Marchantia polymorpha: $_{pro}$Mp*LYK1*:Mp*LYK1*$^{\#2}$/Mp*lyk1-1*^{ko}	This study	N/A
Marchantia polymorpha: $_{pro}$Mp*LYK2*:Mp*LYK2*$^{\#1}$/Mp*lyk2*^{ko}	This study	N/A
Marchantia polymorpha: $_{pro}$Mp*LYK2*:Mp*LYK2*$^{\#2}$/Mp*lyk2*^{ko}	This study	N/A
Marchantia polymorpha: $_{pro}$Mp*LYR*:Mp*LYR*$^{\#1}$/Mp*lyr-1*^{ge}	This study	N/A
Marchantia polymorpha: $_{pro}$Mp*LYR*:Mp*LYR*$^{\#2}$/Mp*lyr-1*^{ge}	This study	N/A
Marchantia polymorpha: $_{pro}$Mp*LYP*:Mp*LYP*$^{\#1}$/Mp*lyp*^{ko}	This study	N/A
Marchantia polymorpha: $_{pro}$Mp*LYP*:Mp*LYP*$^{\#2}$/Mp*lyp*^{ko}	This study	N/A
Marchantia polymorpha: $_{pro}$Mp*LYK1*:Mp*LYK1-mCitrine*/Mp*lyk1-1*^{ko}	This study	N/A
Marchantia polymorpha: $_{pro}$Mp*LYR*:Mp*LYR-mTurquoise2*/Mp*lyr-1*^{ge}	This study	N/A
Marchantia polymorpha: Mp*phot*^{ko}	Komatsu et al.[34]	N/A
Arabidopsis thaliana: Col-8	Widely distributed	N/A
Oligonucleotides		
Oligonucleotides used in this study are listed in Table S1	This study	N/A
Recombinant DNA		
pJHY-TMp1	Ishizaki et al.[49]	N/A
pJHY-TMp1-Mp*LYK1_HR2k*	This study	N/A
pJHY-TMp1-Mp*LYK1_HR4k*	This study	N/A
pJHY-TMp1-Mp*LYK2*	This study	N/A
pJHY-TMp1-Mp*LYP*	This study	N/A
pMpGE_En03	Sugano et al.[50]	RRID: Addgene_71535
pMpGE_En03-Mp*LYRgRNA1*	This study	N/A
pMpGE_En03-Mp*LYRgRNA2*	This study	N/A
pMpGE010	Sugano et al.[50]	RRID: Addgene_71536
pMpGE010-Mp*LYRgRNA1*	This study	N/A
pMpGE010-Mp*LYRgRNA2*	This study	N/A
pENTR4	ThermoFisher	Cat#A10465
pENTR4-$_{pro}$Mp*LYK1*	This study	N/A
pENTR4-$_{pro}$Mp*LYK1*:Mp*LYK1*	This study	N/A
pENTR4-$_{pro}$Mp*LYK2*	This study	N/A
pENTR4-$_{pro}$Mp*LYK2*:Mp*LYK2*	This study	N/A
pENTR4-$_{pro}$Mp*LYR*	This study	N/A
pENTR4-Mp*LYR*	This study	N/A
pENTR4-mMp*LYR*	This study	N/A

(*Continued on next page*)

Please cite this article in press as: Yotsui et al., LysM-mediated signaling in *Marchantia polymorpha* highlights the conservation of pattern-triggered immunity in land plants, Current Biology (2023), https://doi.org/10.1016/j.cub.2023.07.068

Continued

REAGENT or RESOURCE	SOURCE	IDENTIFIER
pENTR4-$_{pro}$MpLYP	This study	N/A
pENTR4-MpLYP	This study	N/A
pMpGWB104	Ishizaki et al.[51]	RRID: Addgene_68558
pMpGWB104-$_{pro}$MpLYK1:GUS	This study	N/A
pMpGWB104-$_{pro}$MpLYK2:GUS	This study	N/A
pMpGWB104-$_{pro}$MpLYR:GUS	This study	N/A
pMpGWB104-$_{pro}$MpLYP:GUS	This study	N/A
pMpGWB301	Ishizaki et al.[51]	RRID: Addgene_68629
pMpGWB301-$_{pro}$MpLYK1:MpLYK1	This study	N/A
pMpGWB301-$_{pro}$MpLYK2:MpLYK2	This study	N/A
*pMpGWB301-$_{pro}$MpLYR:*mMp*LYR*	This study	N/A
pMpGWB301-$_{pro}$MpLYP:MpLYP	This study	N/A
pMpGWB338	Takayuki Kohchi, Kyoto University	N/A
pMpGWB338-$_{pro}$MpLYK1:MpLYK1-mCitrine	This study	N/A
pMpGWB340	Takayuki Kohchi, Kyoto University	N/A
pMpGWB340-$_{pro}$MpLYR:mTurquoise2	This study	N/A
*pMpGWB340-$_{pro}$MpLYR:*mMp*LYR-mTurquoise2*	This study	N/A
Software and algorithms		
NightSHADE LB985	Berthold Technologies	N/A
SpectraMax i3	Molecular Devices	N/A
RNA-Seq library preparation	Kumar et al.[52]	N/A
Illumina Hiseq 4000	BGI	https://www.genomics.cn/
Ghost Koala KEGG	Kanehisa et al.[53]	N/A
Carbohydrate Active Enzyme database (CAZy)	Lombard et al.[54]	N/A
Gene Ontology (GO)	Gene Ontology Consortium[55]	N/A
Kyoto Encyclopedia of Genes and Genomes (KEGG)	Ogata et al.[56]	N/A
EuKaryotic Orthologous Groups (KOG)	Tatusov et al.[57]	N/A
PFAM	Finn et al.[58]	N/A
Panther	Thomas et al.[59]	N/A
MEROPS	Rawlings et al.[60]	N/A
R packages KEGG.db	Carlson[61]	N/A
R packages GO.db	Carlson[62]	N/A
R packages PFAM.db	Carlson et al.[63]	N/A
Fastp	Chen et al.[64]	N/A
STAR	Dobin et al.[65]	N/A
R package DESeq2	Love et al.[66]	N/A
R package pheatmap	Kolde[67]	N/A
SHIN+GO	Miyauchi et al.[68–71]	N/A
R	R Core Team[72]	N/A
Metascape	Zhou et al.[73]	https://metascape.org
agriGO v2.0	Tian et al.[74]	http://systemsbiology.cpolar.cn/agriGOv2/
Geneious 9.1.2 software package	N/A	http://www.geneious.com
MUSCLE	Edgar[75]	N/A
PhyML program ver. 2.2.0	Guindon and Gascuel[76]	N/A
iTOL	N/A	https://itol.embl.de
ZEN2012 software	Carl Zeiss	N/A
LightCycler 96 software version 1.1.0.1320	Roche Diagnostics	N/A
MaxQuant software version 1.6.3.4	Cox and Mann[77]	http://www.maxquant.org/

(*Continued on next page*)

Continued

REAGENT or RESOURCE	SOURCE	IDENTIFIER
Perseus version 1.5.8.5	Tyanova[78]	https://maxquant.net/perseus/
Microsoft Excel v16	Microsoft	N/A
RStudio v2022.12.0+353	N/A	https://www.rstudio.com/
Other		
Marchantia polymorpha genome MpTak1v5.1	MarpolBase, Bowman et al.[22]	https://marchantia.info/download/tak1v5.1/
Arabidopsis thaliana genome TAIR10	Phytozome	https://phytozome-next.jgi.doe.gov/info/Athaliana_TAIR10
Lotus japonicus genome	Miyakogusa.jp 3.0	https://www.kazusa.or.jp/lotus/
Medicago truncatula genome Mt4.0v1	Phytozome	https://phytozome.jgi.doe.gov/pz/portal.html#!info?alias=Org_Mtruncatula
Cuscuta australis genome	Sun et al.[79]	http://groups.english.kib.cas.cn/epb/dgd/Download/201711/t20171101_386248.html
Cuscuta campestris genome	Vogel et al.[80]	https://www.plabipd.de/project_cuscuta2/start.ep
Selaginella moellendorffii genome v1.0	Phytozome, Banks et al.[81]	https://phytozome.jgi.doe.gov/pz/portal.html#!info?alias=Org_Smoellendorffii
Sphagnum fallax genome v0.5	Phytozome	https://phytozome.jgi.doe.gov/pz/portal.html#!info?alias=Org_Sfallax
Physcomitrium patens genome v3.3	Phytozome	https://phytozome.jgi.doe.gov/pz/portal.html#!info?alias=Org_Ppatens
Chara braunii genome	Nishiyama et al.[25]	https://bioinformatics.psb.ugent.be/orcae/overview/Chbra
Spirogyra pratensis transcriptome	Ju et al.[82]	https://www.ncbi.nlm.nih.gov/Traces/wgs/wgsviewer.cgi?val=GBSM01&search=GBSM01000000&display=scaffolds
Nitella mirabilis trancriptome	Ju et al.[82]; Delaux et al.[83]	https://www.ncbi.nlm.nih.gov/Traces/wgs/wgsviewer.cgi?val=GBST01&search=GBST01000000&display=scaffolds

RESOURCE AVAILABILITY

Lead contact

Requests for resources and further information should be directed towards Hirofumi Nakagami (nakagami@mpipz.mpg.de).

Materials availability

Plasmids and plant materials generated in this study are all available upon request. Please note that the distribution of transgenic plants will be governed by material transfer agreements (MTAs) and will be dependent on appropriate import permits acquired by the receiver.

Data and code availability

- RNA-seq data and mass spectrometry data have been deposited to NCBI BioProject and ProteomeXchange Consortium, respectively. The DOI is listed in the key resources table.
- This paper does not report original code.
- Any additional information required to reanalyze the data reported in this paper is available from the lead contact upon request.

EXPERIMENTAL MODEL AND SUBJECT DETAILS

Plant materials and growth condition

Male and female accessions of *M. polymorpha*, Takaragaike-1 (Tak-1) and Takaragaike-2 (Tak-2), respectively were used as wild-type. Plants were grown on 1/2 Gamborg's B5 medium containing 1% agar at 22 °C under 50–60 μmol photons $m^{-2}s^{-1}$ continuous white fluorescent light. Six-day-old gemmalings (cultured mature gemmae) in liquid 1/2 Gamborg's B5 medium containing 0.1% sucrose with shaking at 130 rpm were used for the ROS assay, MAP kinase assay, RT-PCR, and quantitative RT-PCR (qRT-PCR).

Please cite this article in press as: Yotsui et al., LysM-mediated signaling in *Marchantia polymorpha* highlights the conservation of pattern-triggered immunity in land plants, Current Biology (2023), https://doi.org/10.1016/j.cub.2023.07.068

METHOD DATAILS

ROS assay

Four 6-day-old gemmalings were incubated in water containing 100 μM 8-amino-5-chloro-7-phenylpyrido [3,4-d] pyridazine-1,4-(2H,3H) (L-012) (Wako, Japan) for 2 hours at 22 °C under darkness, followed by transfer to water containing different elicitors. ROS production was determined by counting photons derived from L-012-mediated chemiluminescence using NightSHADE LB985 (Berthold Technologies, Germany) or SpectraMax i3 (Molecular Devices, USA).

MAP kinase assay

Twenty to thirty 6-day-old gemmalings were treated with 1 μg/ml N-acetylchitooctaose (GN8) or mock, then proteins were extracted using extraction buffer (50 mM Tris-HCl (pH 7.5), 10 mM $MgCl_2$, 15 mM EGTA, 100 mM NaCl, 2 mM DTT, 1 mM sodium fluoride, 0.5 mM Na_3VO_4, 30 mM β-glycerophosphate, 0.1% (v/v) NP-40, and cOmplete protease inhibitor cocktail EDTA-free tablet (Roche, Germany)). Phosphorylated MAPK proteins were detected by immunoblot analysis with antiphospho-p44/42 MAPK (Erk1/2)(Thr202/Tyr204) (D13.14.4E) rabbit mAb (Cell Signaling Technology, USA). The blotted membrane was stained with Coomassie Brilliant blue (CBB) to verify equal loading.

RNA-seq analysis

Twenty to thirty 9-day-old Tak-2 and Mp*phot*^{ko} plants were transferred to petri dishes with water and incubated for one day and then harvested without treatment (0 hr) or treated with 1 μM N-acetylchitoheptaose (GN7) for 1, 3, 24 hours or with mock for 1, 3, 24 hours. Thirty-five 8-day-old *A. thaliana* Col-8 seedlings, which were cultured in 1/2 MS liquid medium containing 0.1% sucrose at 22 °C under 50–60 μmol photons $m^{-2}s^{-1}$ long day condition, were transferred to petri dishes with water and incubated for one day and then harvested without treatment or treated with 100 μM N-acetylchitoheptaose (GN7) for 1, 3, 24 hours or with mock for 1, 3, 24 hours. RNA-Seq library preparation was carried out using a high-throughput RNA-Seq method.[52] The 100-bp paired-end reads were sequenced on an Illumina Hiseq 4000 platform by BGI (https://www.genomics.cn/). The *M. polymorpha* genome files were obtained from MarpolBase (MpTak1v5.1; https://marchantia.info/download/tak1v5.1/). We combined functional annotations from JGI Phytozome (https://genome.jgi.doe.gov/portal/) and Ghost Koala KEGG.[53] The genome files of *A. thaliana* were obtained from JGI Phytozome. The following functional annotation sets were combined for the analyses, Carbohydrate Active Enzyme database (CAZy;[54]), the Gene Ontology (GO;[55]), Kyoto Encyclopedia of Genes and Genomes (KEGG;[56]), and EuKaryotic Orthologous Groups (KOG;[57]), PFAM,[58] Panther,[59] and MEROPS.[60] MEROPS and GO terms were obtained based on KEGG, GO, PFAM, IDs using R packages KEGG.db,[61] GO.db,[62] and PFAM.db.[63] The raw reads were quality-trimmed using Fastp with default parameters.[64] We performed mapping reads and counting transcripts per gene with the *A. thaliana* and *M. polymorpha* genomes using STAR.[65] The log_2 fold difference of the gene expression between conditions was calculated with R package DESeq2.[66] The genes with very low count were excluded (less than 10 reads summed from all conditions) for the analyses. Genes with statistical significance were selected (FDR adjusted $p < 0.05$). Normalized read counts of the genes were also produced with DESeq2, which were subsequently log_2 transformed. Differentially expressed genes were grouped using K-means clustering with R package, pheatmap.[67] All procedures were orchestrated with the visual pipeline SHIN+GO.[68–71] R was used for operating the pipeline.[72] The RNA-seq data used for this study are available under NCBI BioProject PRJNA917430. The gene ontology (GO) enrichment analysis for DEGs was performed by Metascape (https://metascape.org)[73] or agriGO v2.0 (http://systemsbiology.cpolar.cn/agriGOv2/).[74] For GO analysis of DEGs in *M. polymorpha*, the best BLASTP hit genes in *A. thaliana* was used (Best.hit.arabi.name_v3.1 in Data S1M, S1S, and S1T).

Database search

Amino acid sequences of LysM receptor homologs were obtained from the following databases: https://phytozome-next.jgi.doe.gov/info/Athaliana_TAIR10 for *Arabidopsis thaliana*, https://www.kazusa.or.jp/lotus/ for *Lotus japonicus*, https://phytozome.jgi.doe.gov/pz/portal.html#!info?alias=Org_Mtruncatula for *Medicago truncatula*, http://groups.english.kib.cas.cn/epb/dgd/Download/201711/t20171101_386248.html for *Cuscuta australis*, https://www.plabipd.de/project_cuscuta2/start.ep for *Cuscuta campestris*, https://phytozome.jgi.doe.gov/pz/portal.html#!info?alias=Org_Smoellendorffii for *Selaginella moellendorffii*, https://phytozome.jgi.doe.gov/pz/portal.html#!info?alias=Org_Sfallax for *Sphagnum fallax*, https://phytozome.jgi.doe.gov/pz/portal.html#!info?alias=Org_Ppatens for *Physcomitrium patens*, https://marchantia.info/download/tak1v5.1/ for *Marchantia polymorpha*, and https://bioinformatics.psb.ugent.be/orcae/overview/Chbra for *Chara braunii*, https://www.ncbi.nlm.nih.gov/Traces/wgs/wgsviewer.cgi?val=GBSM01&search=GBSM01000000&display=scaffolds for *Spirogyra pratensis*, and https://www.ncbi.nlm.nih.gov/Traces/wgs/wgsviewer.cgi?val=GBST01&search=GBST01000000&display=scaffolds for *Nitella mirabilis*. The *LysM* genes in *Oryza sativa* were previously described.[15,16] The *LysM* gene in *Nitella mirabilis* was previously described.[83]

Phylogenetic analysis of LysM receptor homologs

Alignment of full-length proteins was constructed using MUSCLE alignment[75] implemented in the Geneious 9.1.2 software package (Biomatters; http://www.geneious.com) at the default parameters, and then LysM1, LysM2, and LysM3 domains, which were previously defined,[84] were extracted from the full-length protein alignment. An unrooted or rooted maximum-likelihood phylogenetic tree was constructed using PhyML program ver. 2.2.0[76] implemented in the Geneious software, using the LG as substitution model.

Please cite this article in press as: Yotsui et al., LysM-mediated signaling in *Marchantia polymorpha* highlights the conservation of pattern-triggered immunity in land plants, Current Biology (2023), https://doi.org/10.1016/j.cub.2023.07.068

Genomic DNA extraction

Total DNA was extracted from approximately 1 g of fresh weight of 6-day-old gemmalings using the cetyl trimethyl ammonium bromide (CTAB) method as previously described[85] or using ISOPLANT II (Nippon Gene, Japan).

RNA extraction and cDNA synthesis

Total RNA was extracted from 6-day-old gemmalings using the RNeasy Plant Mini Kit (QIAGEN, Netherlands) or NucleoSpin RNA Plant (Macherey-Nagel, Germany). First-strand complementary DNA was synthesized from 0.5 μg total RNA using a ReverTra Ace qPCR RT Master Mix with gDNA Remover (Toyobo, Japan).

Plasmid constructions and transformation

The 5 kbp putative promoter fragment upstream of the translation initiation codon of each gene was cloned into pENTR4 dual-selection vector (Thermo Fisher Scientific, USA) using an In-Fusion HD cloning kit, and then they were subcloned into binary vector pMpGWB104[51] for constructing $_{pro}$Mp*LYK1:GUS*, $_{pro}$Mp*LYK2:GUS*, $_{pro}$Mp*LYR:GUS*, and $_{pro}$Mp*LYP:GUS* using LR clonase II enzyme mix (Thermo Fisher Scientific, USA). To generate the targeting vectors for Mp*lyk1-1*^{ko}, Mp*lyk1-2*^{ko}, Mp*lyk2*^{ko}, and Mp*lyp*^{ko}, homologous arms were amplified from Tak-1 genomic DNA using KOD Plus Neo (Toyobo, Japan). The PCR-amplified fragments of the 5' end and 3' end were cloned into the *Pac*I site and *Asc*I site of pJHY-TMp1,[49] respectively, using an In-Fusion HD cloning kit (Clontech Laboratories, USA). Targeting vectors were introduced into F1 sporelings of *M. polymorpha* derived from crosses between Tak-1 and Tak-2, as described previously.[86] To generate the targeting vectors for Mp*lyr-1*^{ge}, Mp*lyr-2*^{ge}, and Mp*lyr-3*^{ge}, annealed oligos for an Mp*LYR*-targeting gRNA1 and an Mp*LYR*-targeting gRNA2 were ligated into *Bsa*I-digested pMpGE_En03[50] using an T4 DNA ligase (NEB, UK). Mp*lyr-1*^{ge} was generated using Mp*LYR*-targeting gRNA1. Mp*lyr-2*^{ge} was generated using both Mp*LYR*-targeting gRNA1 and gRNA2. Mp*lyr-3*^{ge} was generated using Mp*LYR*-targeting gRNA2. Mp*LYR*-targeting gRNAs were subcloned into binary vector pMpGE010[50] using LR clonase II enzyme mix. Screening for homologous recombination-mediated gene-targeted lines was performed by genomic PCR as described previously.[49] Screening for CRISPR/Cas9-mediated targeted mutagenesis lines was performed by genomic PCR as described previously.[87] The open reading frame (ORF) fragment of Mp*LYK1* and Mp*LYK2* was cloned into corresponding pENTR4-promoter, and then they were subcloned into binary vector pMpGWB301[51] for constructing $_{pro}$Mp*LYK1:*Mp*LYK1* and $_{pro}$Mp*LYK2:*Mp*LYK2*. The ORF fragment of Mp*LYP* was cloned into pENTR4. The ORF fragment of Mp*LYR* was cloned into pENTR4, then the PAM sequence of Mp*LYR* in pENTR4-Mp*LYR* was mutated, as shown in Figure S5D, using PrimeSTAR® Mutagenesis Basal Kit (Takara, Japan) so as not to be targeted by CRISPR/Cas9. pENTR4-$_{pro}$Mp*LYP* and pENTR4-$_{pro}$Mp*LYR* were subcloned into binary vector pMpGWB301, and then the ORF fragment of Mp*LYP* and mMp*LYR* was cloned into the corresponding pMpGWB301-promoter for constructing $_{pro}$Mp*LYP:*Mp*LYP* and $_{pro}$Mp*LYR:*mMp*LYR*. The resultant plasmids were introduced into corresponding knockout mutants, as described previously.[49] Primers used are listed in Table S1 (No. 1-46).

Assays for GUS activity and sectioning

Histochemical GUS assays were performed according to the reported method[88] with some modifications, as previously described.[89] For sectioning, GUS-stained samples were embedded into Technovit 7100 resin according to the manufacturer's instructions (Heraeus Kulzer). Embedded samples were then sectioned into 10 μm-thick sections using RM2125 RTS microtome (Leica, Germany) or RV-240 microtome (Yamato, Japan) with TC-65 tungsten blade.

Confocal laser scanning microscopy

Five-day-old gemmalings grown on 1/2 Gamborg's B5 medium containing 1% (w/v) sucrose and 1% (w/v) agar at 22 °C under continuous white light were used for observation. The samples were mounted in a 1/2 Gamborg's B5 liquid medium and observed using an LSM780 confocal microscope (Carl Zeiss, Germany) equipped with an oil immersion lens (63×, numerical aperture = 1.4). The plant expressing MpLYK1-mCitrine was excited at 488 nm (Argon) and 561 nm (DPSS 561-10), and emissions between 482–659 nm were collected. The plant expressing MpLYR-mTurquoise2 was excited at 405 nm (Diode 405-30)), and emissions between 428–659 nm were collected. Spectral unmixing of the obtained images was conducted using ZEN2012 software (Carl Zeiss, Germany).

Quantitative RT-PCR or semi quantitative RT-PCR

Quantitative RT-PCR was performed using a LightCycler 96 (Roche, Switzerland). Thunderbird SYBR qPCR Mix (Toyobo, Japan) was used for amplification. Mp*EF1α* was used as an internal standard. Semi quantitative RT-PCR was performed using a thermal cycler. Mp*ACT1* was used as an internal standard. Primers used for qRT-PCR and semi qRT-PCR are listed in Table S1 (No. 47-90).

Bioluminescence-based bacteria quantification

Bacterial quantification in infected thalli was carried out as described before.[48] Briefly, *M. polymorpha* were grown on autoclaved cellophane disc on 1/2 Gamborg's B5 medium for two weeks. In the meantime, *Pto*-lux was cultivated in King's B medium containing 30 μg/mL rifampicin to achieve an OD_{600} of 1.0. The saturated bacterial culture was subsequently washed and resuspended in Milli-Q water to prepare a bacterial suspension with of an OD_{600} of 1.0. Next, 2-week-old thalli were submerged in the bacterial suspension followed by vacuum for 5 min and incubation for 0 to 3 days on pre-wetted filter papers. After incubation, thallus discs (5 mm

Please cite this article in press as: Yotsui et al., LysM-mediated signaling in *Marchantia polymorpha* highlights the conservation of pattern-triggered immunity in land plants, Current Biology (2023), https://doi.org/10.1016/j.cub.2023.07.068

diameter) were punched from the basal region using a sterile biopsy punch (pfm medical) and transferred to a 96-well plate (VWR, USA). Bioluminescence was measured in a FLUOstar Omega plate reader (BMG Labtech, Germany).

Fusarium oxysporum infection assay

The tomato pathogenic isolate *Fusarium oxysporum* (*Fo*) f.sp. *lycopersici* 4287 (Fol4287) was used in this study, which has been previously described.[28] For infection assays, *M. polymorpha* gemmae were plated on Whatman circular filter papers placed on 1/2 Gamborg's B5 1% agar plates for three weeks. Dip inoculation of plants was performed by submerging the filters into a suspension of *Fo* microconidia (5 x 10^5 spores ml^{-1}) for 30 minutes. Filters were then transferred to pots containing vermiculite, and thallus tissue was collected from five independent plants and frozen in liquid nitrogen at appropriate time points. DNA was extracted using CTAB chloroform:octanol protocol as previously described.[28] Quantification of fungal DNA was performed using a Quantstudio 5 Real-Time PCR system (Applied Biosystems, USA) with oligos targeting the *Fo* gene *six1* (Fol4287-specific), and normalized to the *M. polymorpha* housekeeping gene Mp*EF1*α as previously described.[28] The data represent the ratio of expression levels (relative fungal biomass) compared to *Fo*-infected Tak-1 control plants.

Phosphoproteome analysis

Seven to 10-day-old Tak-1, Tak-2, or Mp*lyk1-1*^{ko} gemmalings, which were cultured in 1/2 Gamborg's B5 liquid medium containing 0.1% sucrose, were transferred to petri dishes with water. For chitin treatment experiment (Data S1D–S1G and S1U–S1Y), transferred gemmalings were incubated overnight at room temperature. Then gemmalings were treated with 1 μM N-acetylchitoheptaose (GN7), 1 μg/ml N-acetylchitooctaose (GN8), or mock for 10 min at room temperature and then immediately frozen with liquid nitrogen. For blue-light or chitin treatment experiment (Data S1H–S1L), transferred gemmalings were incubated in the dark at 22 °C for 3 days. Then gemmalings were treated with 1 μg/ml N-acetylchitooctaose (GN8) or mock for 10 min in dark condition or irradiated with blue-light (90 μmol $m^{-2}s^{-1}$) (MIL-B18, SANYO Electric, Japan) for 10 min at room temperature and then immediately frozen with liquid nitrogen. For Data S1D–S1L, sample preparation and liquid chromatography-tandem mass spectrometry (LC–MS/MS) analysis was performed as described previously with minor modifications.[90] For Data S1U–S1Y, samples were analyzed using an Ultimate 3000 RSLC nano (Thermo Fisher Scientific, USA) coupled to an Orbitrap Exploris 480 mass spectrometer equipped with a FAIMS (field asymmetric ion mobility separation) Pro interface (Thermo Fisher Scientific, USA). Peptides were concentrated on an Acclaim PepMap 100 pre-column (75 μM x 2 cm, C18, 3 μM, 100 Å, Thermo Fisher Scientific, USA) with a flow of 15 μl/min (0.1% trifluoroacetic acid (TFA)) for 5 min using the loading pump. Peptides were separated on 16 cm frit-less silica emitters (75 μm inner diameter, New Objective, USA) packed in-house with reversed-phase ReproSil-Pur C18 AQ 1.9 μm resin (Dr. Maisch, Germany). Peptides were loaded on the column and eluted for 130 min using a segmented linear gradient of 5% to 95% solvent B (0 min 5% B, 0–5 min → 5% B, 5–65 min → 20% B, 65–90 min → 35% B, 90–100 min → 55% B, 100–105 min → 95% B, 105–115 min → 95% B, 115–115.1 min → 5% B, 115.1–130 min 5% B) (solvent A: 0% ACN, 0.1% formic acid (FA); solvent B: 80% ACN, 0.1%FA) at a flow rate of 300 nl/min. Mass spectra were acquired in data-dependent acquisition (DDA) mode with a TOP_S method using a cycle time of 2 seconds. For FAIMS, two compensation voltages (-45 and -65) were applied. The cycle time for CV-45 and CV-65 was set to 1.2 seconds and 0.8 seconds, respectively. In addition to DDA, a target list for the phosphopeptides FSTQSVVALPLEGSQSAK [1p], SAAEDALAAAGIRPSQILSPSGSGR [2p], and PSQILSPSGSGR [2p] was used. The instrument performed DDA scans if no targets were found. MS spectra were acquired in the Orbitrap analyzer with a mass range of 320–1200 m/z at a resolution of 60,000 FWHM and a normalized AGC target of 300%. Precursors were filtered using the MIPS option (MIPS mode = peptide), the intensity threshold was set to 5,000. Precursors were selected with an isolation window of 1.6 m/z. HCD fragmentation was performed at a normalized collision energy of 30%. MS/MS spectra were acquired with a target value of 75% ions at a resolution of 15,000 FWHM, at an injection time of 120 ms and a fixed first mass of m/z 120. Peptides with a charge of +1, greater than +6, or with unassigned charge state were excluded from fragmentation for MS/MS. Raw data were processed using MaxQuant software (version 1.6.3.4, http://www.maxquant.org/)[77] with label-free quantification (LFQ) and iBAQ enabled.[91] MS/MS spectra were scanned by the Andromeda search engine against a combined database containing the sequences from *M. polymorpha* (MpTak1v5.1_r1.protein.fasta, https://marchantia.info/download/tak1v5.1/), sequences of 248 common contaminant proteins, and decoy sequences. Trypsin specificity was required and a maximum of two missed cleavages allowed. Minimal peptide length was set to seven amino acids. Carbamidomethylation of cysteine residues was set as fixed, phosphorylation of serine, threonine and tyrosine, oxidation of methionine and protein N-terminal acetylation as variable modifications. The match between runs option was enabled. Peptide-spectrum-matches and proteins were retained if they were below a false discovery rate of 1% in both cases. Statistical analysis of the intensity values obtained for the phospho-modified peptides ("modificationSpecificPeptides.txt" output file) was carried out using Perseus (version 1.5.8.5, http://www.maxquant.org/). Intensities were filtered for reverse and contaminant hits and the data was filtered to retain only phospho-modified peptides. Next, intensity values were $\log_2$ transformed. After grouping samples by condition only those sites were retained for the subsequent analysis that had four valid values in one of the conditions in case of GN8 vs mock analysis (Data S1D–S1G) and two valid values in one of the conditions in case of GN8, blue-light, mock analysis (Data S1H–S1L) and Tak-1 vs Mp*lyk1-1*^{ko} analysis (Data S1U–S1Y). Two-sample t-tests were performed using a permutation-based FDR of 0.05. Alternatively, the valid value-filtered data was median-normalized and missing values were imputed from a normal distribution, using the default settings in Perseus (1.8 downshift, separately for each column). The Perseus output was exported and further processed using Excel and RStudio. The MS proteomics data have been deposited in the ProteomeXchange Consortium via the PRIDE partner repository with the dataset identifiers PXD038903, PXD038907, and PXD042084.

Please cite this article in press as: Yotsui et al., LysM-mediated signaling in *Marchantia polymorpha* highlights the conservation of pattern-triggered immunity in land plants, Current Biology (2023), https://doi.org/10.1016/j.cub.2023.07.068

QUANTIFICATION AND STATISTICAL ANALYSIS

MS Excel, R (4.1.0), and RStudio were used for statistical analysis and drawing figures. Bacterial growth, ROS production, RT-qPCR, and fungal biomass quantification was statistically analyzed using Student's t-test, with p-values adjusted by the Benjamini and Hochberg (BH) method. In Figure S6, Statistical analysis of ROS production was performed using the Tukey-HSD test. Statistically significant differences were defined as values with $p < 0.05$.